LOMONOSOV MOSCOW STATE UNIVERSITY

National Center FOR PHYSICS AND MATHEMATICS

Status of tritium neutrino experiment in Sarov

Konstantin Kouzakov

Lomonosov Moscow State University
&
National Center for Physics and Mathematics

XXI Lomonosov Conference on Elementary Particle Physics
24-30 August 2023, Moscow, Russia

The **Sarov tritium neutrino experiment** is a part of the research program of the **National Center for Physics and Mathematics** founded in 2021

The main goals of the experiment are

- **first observation of coherent elastic neutrino-atom scattering (CEνAS)**
- **search for neutrino magnetic moment**

using a high-intensity tritium neutrino source: at least 1 kg, possibly up to 4 kg of tritium

OUTLINE

- ✓ Physics introduction
  - CEνAS
  - neutrino magnetic moment μ_ν
- ✓ He II detector concept
  - observe CEνAS channel & search for μ_ν
- ✓ Si and CsI detector concepts
  - search for μ_ν with atomic ionization channel
- ✓ Summary and outlook

CEνAS: Coherent Elastic Neutrino-Atom Scattering

Yu. V. Gaponov and V. N. Tikhonov,
Elastic scattering of low energy neutrinos by atomic systems,
Yad. Fiz. (USSR) ***26*** *(1977) 594 (in Russian).*

Abstract. Elastic scattering of low energy neutrinos by atomic systems is treated. For the *V* variant of weak interaction scattering on the total system (on electrons, protons and neutrons) is coherent; for the *A* variant neutrino scatters coherently on using simple atomic systems. The result for an arbitrary atom is presented. The analysis shows that at neutrino energies $\lesssim 10$ keV a region of coherent optical neutrino phenomena exists where the neutrino elastic scattering by an atom as a whole dominates.

So far there is no corresponding experimental observation. An experimental study of CEνAS could provide a unique test of the SM neutrino interactions at very low energies.

CEνAS vs CEνNS

CEνNS: Coherent Elastic Neutrino-Nucleus Scattering

predicted by *D. Z. Freedman, PRD **9** (1974) 1389;*
*V. B. Kopeliovich & L. L. Frankfurt, ZhETF Pis. Red. **19**, No. 4 (1974) 236*

observed by *D. Akimov et al. (COHERENT Collab.), Science **357** (2017) 1123*

CEνNS

- $|\vec{q}|R_{\rm nuc} \ll 1$

$\vec{q}$ is the momentum transfer

$R_{\rm nuc}$ is the nuclear radius

CEνAS

- $|\vec{q}|R_{\rm atom} \ll 1$

$R_{\rm atom}$ is the atomic radius

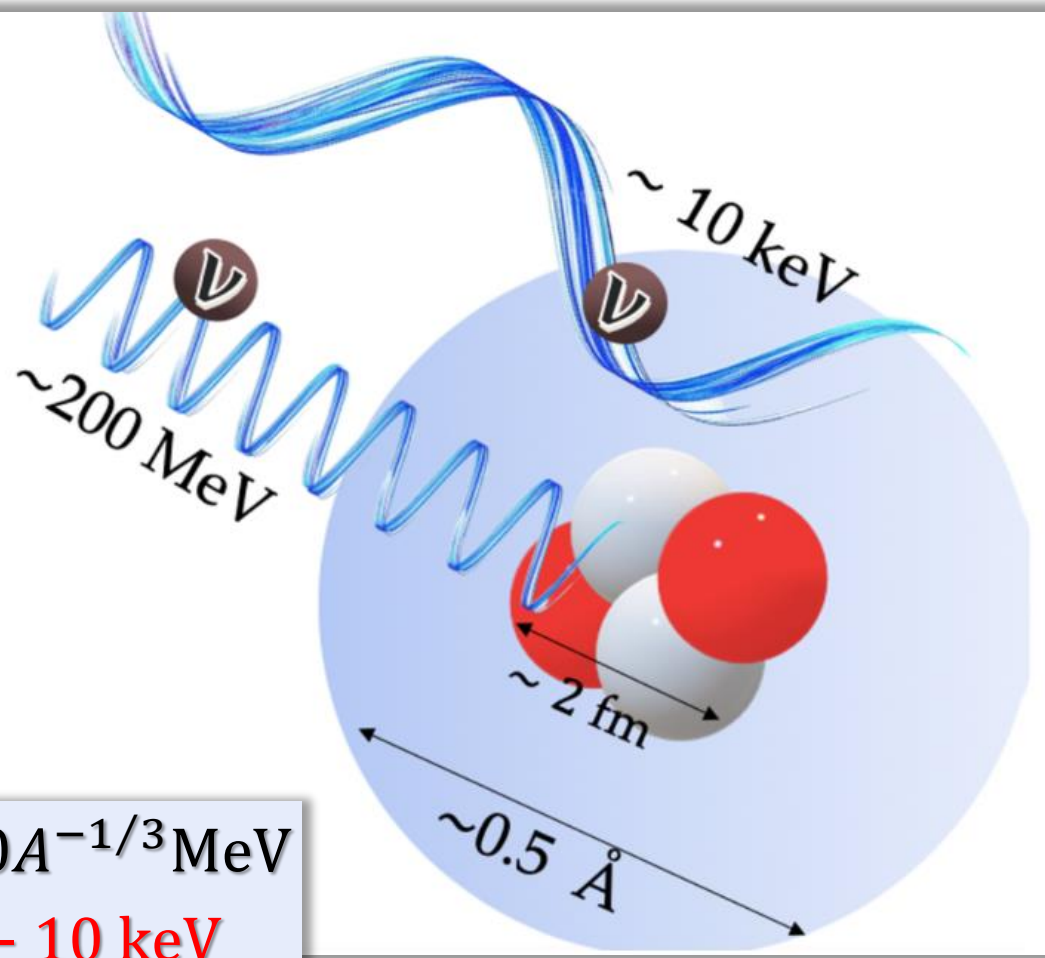

CEνNS: $E_\nu \lesssim 1/R_{\rm nuc} \sim 200A^{-1/3}\,\mathrm{MeV}$

CEνAS: $E_\nu \lesssim 1/R_{\rm atom} \sim 1-10\,\mathrm{keV}$

Global map of CEνNS experiments

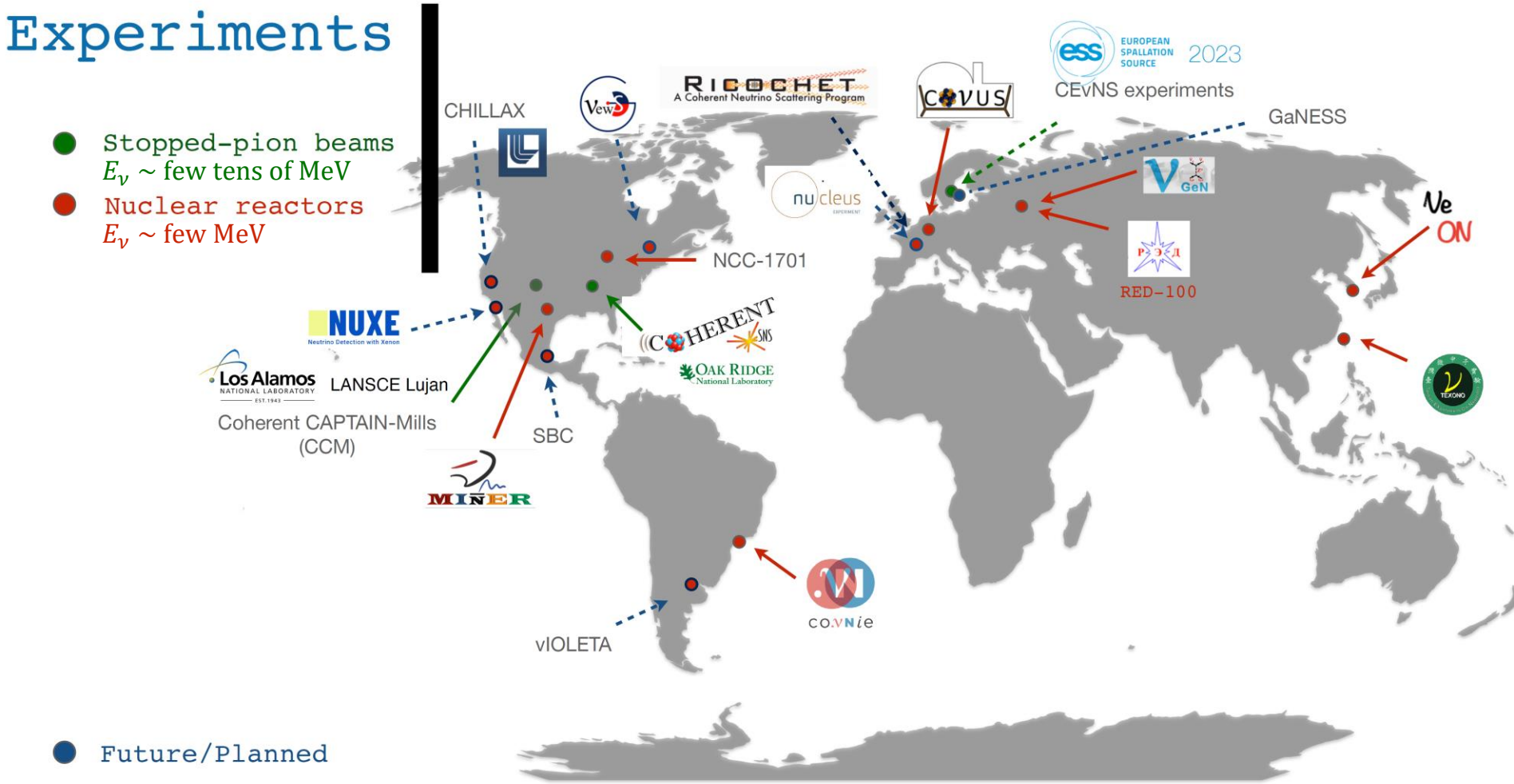

[C. Bonifazi, Neutrino 2022]

Tritium neutrinos

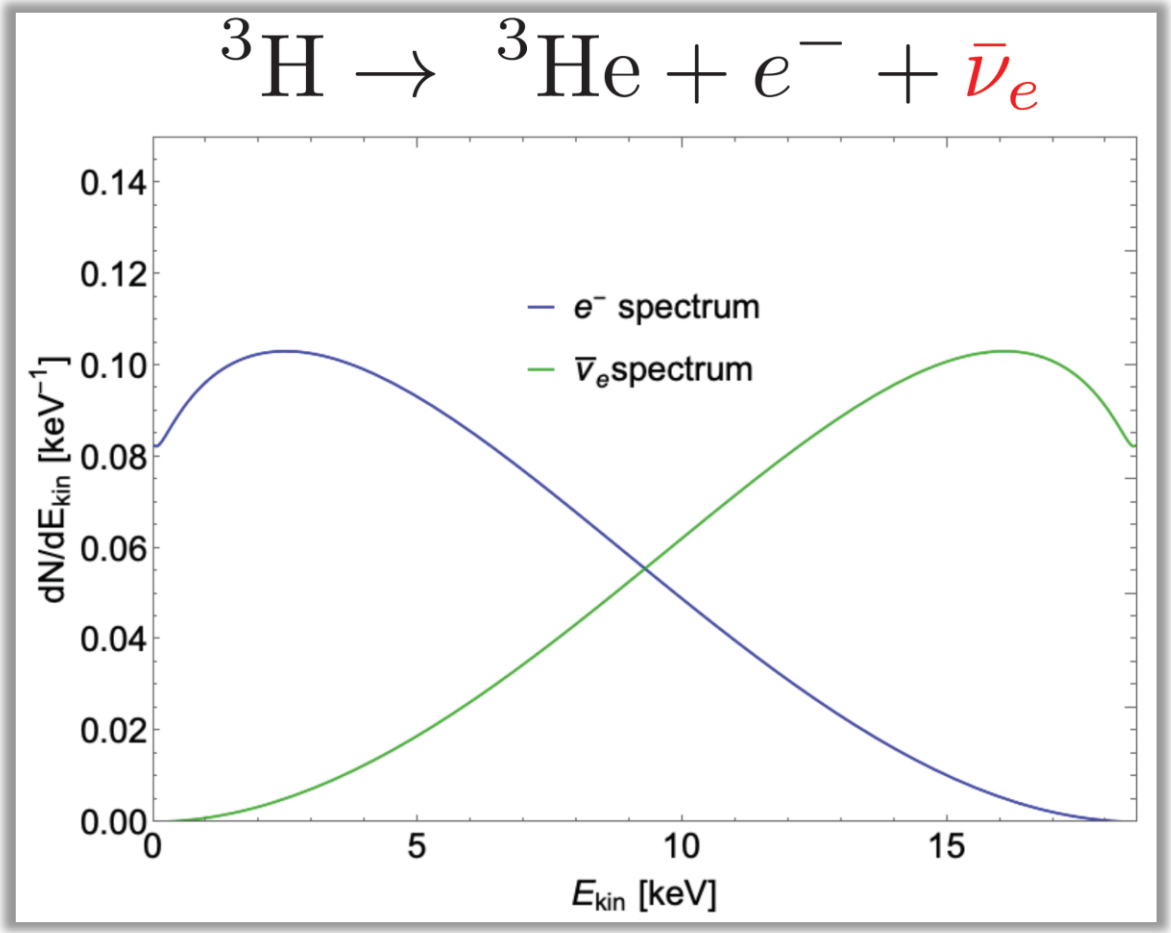

$$Q = 18.6 \text{ keV}$$

$$t_{1/2} = 12.3 \text{ yrs}$$

$$\langle E_{\bar{\nu}_e} \rangle = 12.9 \text{ keV}$$

In contrast to stopped-pion beams ($\langle E_\nu \rangle \sim 30$ MeV) and nuclear reactors ($\langle E_\nu \rangle \sim 1$ MeV), with a tritium neutrino source it is possible to fulfill the coherence condition in elastic neutrino-atom scattering

Atomic recoil energy scale in CEνAS

From energy-momentum conservation it follows that

$$T \leq \frac{2E_\nu^2}{m}$$

T is energy transfer, or atomic recoil energy

m is atomic mass, $m \approx A$ GeV

If E_ν~10 keV: $T \lesssim \frac{200}{A}$ meV

For the lightest atom (A=1): $T \lesssim 200$ meV

Light atomic targets, such as H or He, are needed to observe CEνAS

Proposals for light dark matter searches with He II

SPICE/HeRALD [*R. Anthony-Petersen et al., arXiv:2307.11877v1 [physics.ins-det]*]

DELight [*B. von Krosigk et al., arXiv:2209.10950v1 [hep-ex]*]

Advantages of superufluid He target:

- extreme intrinsic radiopurity
- high impedance to external vibration noise
- unique "quantum evaporation" signal channel enabling the detection of quasiparticle modes (rotons and phonons) via liberation of ^{4}He atoms into a vacuum

*S.A. Hertel et al., PRD **100** (2019) 092007*

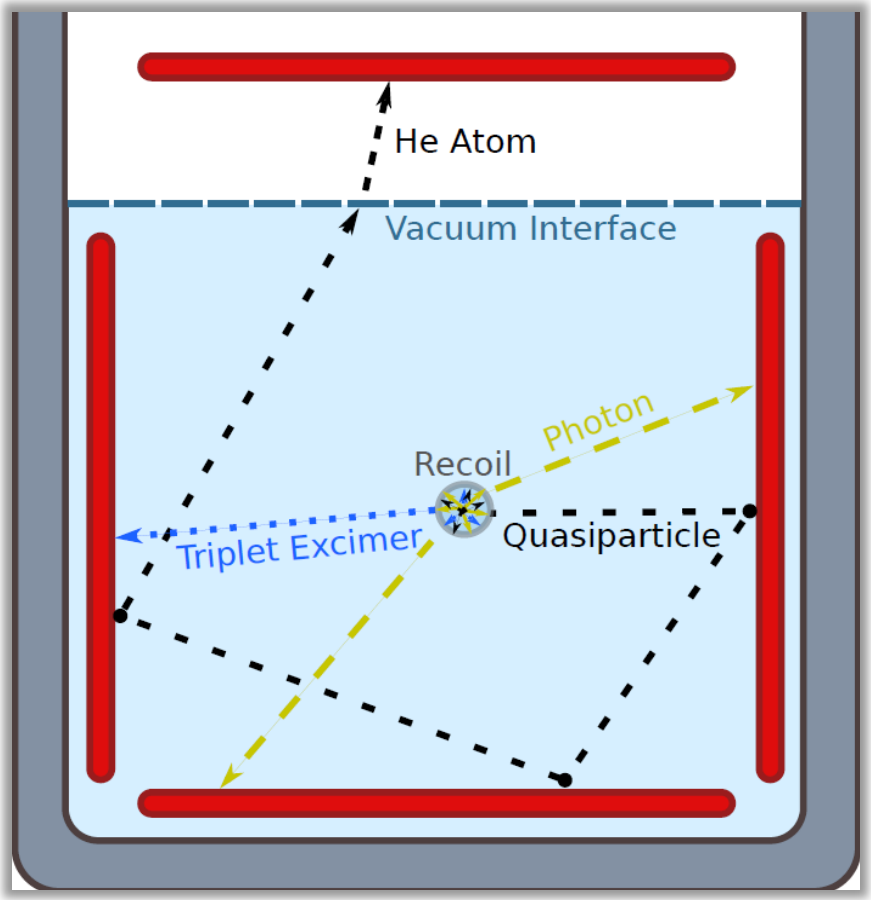

Fig. Simplified detector layout

He-4 atomic recoil spectrum with tritium $\bar{\nu}_e$

*M. Cadeddu, F. Dordei, C. Giunti, K. Kouzakov, E. Picciau, A. Studenikin, PRD **100** (2019) 073014*

$$\frac{d\sigma_{\rm SM}}{dT_R} = \frac{G_F^2 m}{\pi}\left[Z\left(\tfrac{1}{2} - 2\sin^2\theta_W\right) - \tfrac{1}{2}N + Z\left(\tfrac{1}{2} + 2\sin^2\theta_W\right)F_{\rm el}(q^2)\right]^2\left(1 - \frac{mT_R}{2E_\nu^2}\right)$$

$$\frac{d\sigma_{\mu_\nu}}{dT_R} = \frac{\pi\alpha^2 Z^2}{m_e^2}|\mu_\nu|^2\left(\frac{1}{T_R} - \frac{1}{E_\nu}\right)[1 - F_{\rm el}(q^2)]^2 \qquad \text{with} \quad q^2 = 2mT_R$$

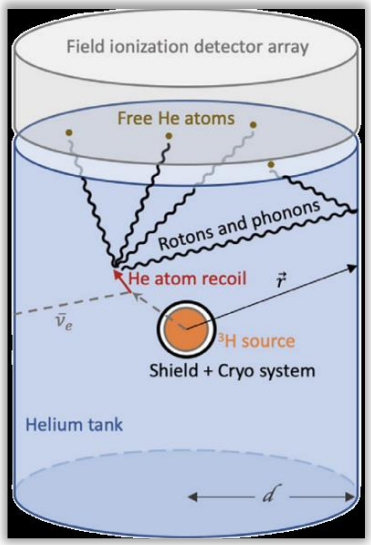

500 kg of helium
60 g of tritium
5 yrs of taking data

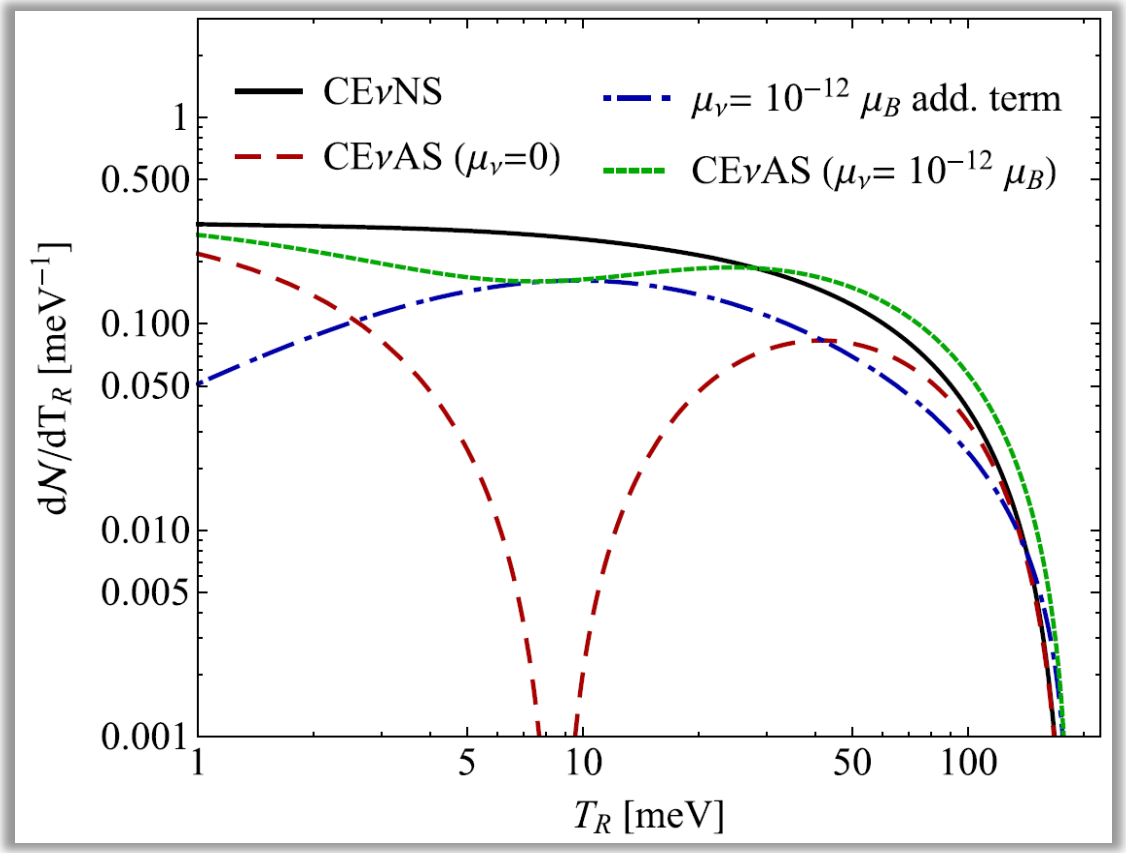

Why neutrino magnetic moment?

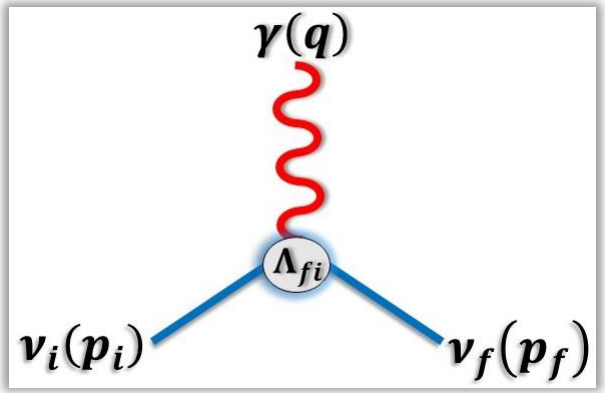

C. Giunti and A. Studenikin,
Neutrino electromagnetic interactions:
A window to new physics,
Rev. Mod. Phys. ***87*** *(2015) 531;*
arXiv:1403.6344

The effective neutrino electromagnetic vertex under the Lorentz and gauge invariance:

$$\Lambda_{\mu}^{(\mathrm{EM};\nu)fi}(q) = \left(\gamma_\mu - \frac{q_\mu q}{q^2}\right)\left[f_Q^{fi}(q^2) - q^2 f_A^{fi}(q^2)\gamma_5\right] - i\sigma_{\mu\nu}q^\nu\left[f_M^{fi}(q^2) + i f_E^{fi}(q^2)\gamma_5\right]$$

In the minimally extended SM with addition of right-handed massive Dirac neutrinos:

$$\mu_\nu \simeq 3.2 \times 10^{-19}\mu_B\left(\frac{m_\nu}{1\ \mathrm{eV}}\right)$$

K. Fujikawa and R. Shrock,
PRL ***45*** *(1980) 963*

$m_\nu < 0.8$ eV at 90% CL
M. Aker et al. (The KATRIN Collaboration),
Nature Physics ***18*** *(2022) 160*

Much greater μ_ν values are predicted beyond the minimally extended SM

World leading upper bounds on μ_ν

Laboratory bounds (elastic $\nu - e^-$ scattering)

solar neutrinos (XENONnT)

*A. Khan, Phys. Lett. B **837** (2023) 137650*

$\mu_\nu < 6.3\times10^{-12}\,\mu_B$

reactor neutrinos (GEMMA)

*A. Beda et al., Adv. High Energy Phys. **2012** (2012) 350150*

$\mu_{\nu_e} < 2.9\times10^{-11}\,\mu_B$

CEνNS bounds

*V. De Romeri et al., JHEP **04** (2023) 035*

$\mu_{\nu_e} < 3.8\times10^{-9}\,\mu_B$

$\mu_{\nu_\mu} < 2.6\times10^{-9}\,\mu_B$

Astrophysical bounds (luminosity of globular cluster stars)

*N. Viaux et al., Astron. & Astrophys. **558** (2013) A12; S. Arceo-Diaz et al, Astropart. Phys. **70** (2015) 1; F. Capozzi and G. Raffelt, Phys. Rev. D **102** (2020) 083007*

$\mu_\nu < (1.2-2.6)\times10^{-12}\,\mu_B$

With CEνAS, we could improve the CEνNS limits by four orders of magnitude, and the world leading limits by an order of magnitude

He II detector concept to study CEνAS

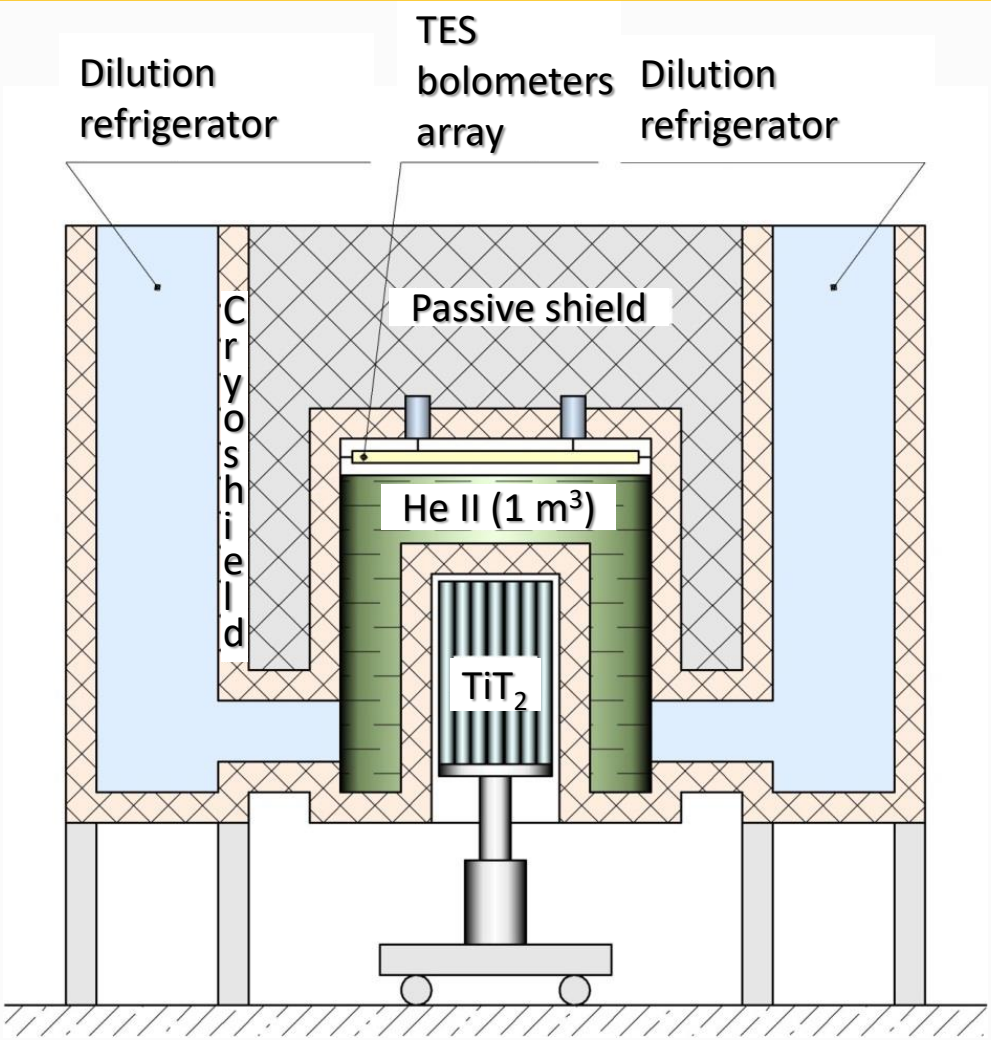

Tritium neutrino source

(1-4 kg, 10-40 MCi)

- Tubular copper elements with TiT_2

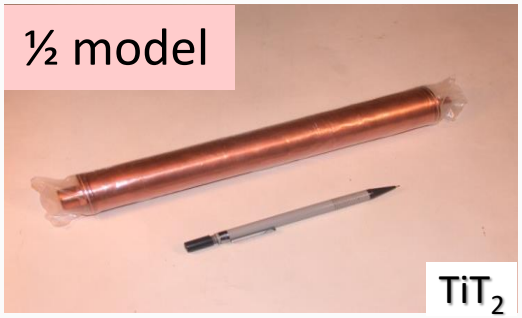

Helium II detector (1000 L)

- Liquid He-4 at 40-60 mK
- Array of ~1000 TESs (transition edge sensors)
- ~1000-channel SQUID readout

Expected results after 5 years of data collection

Number of CEνAS events within SM: **~60 for 1 kg of T_2** and **~200 for 4 kg of T_2**

Sensitivity to neutrino magnetic moment: μ_ν **~ (2-4)x10^{-13} μ_B** at 90% C.L.

Low-background neutrino laboratory in Sarov

@ All-Russian Research Institute of Experimental Physics, RFNC

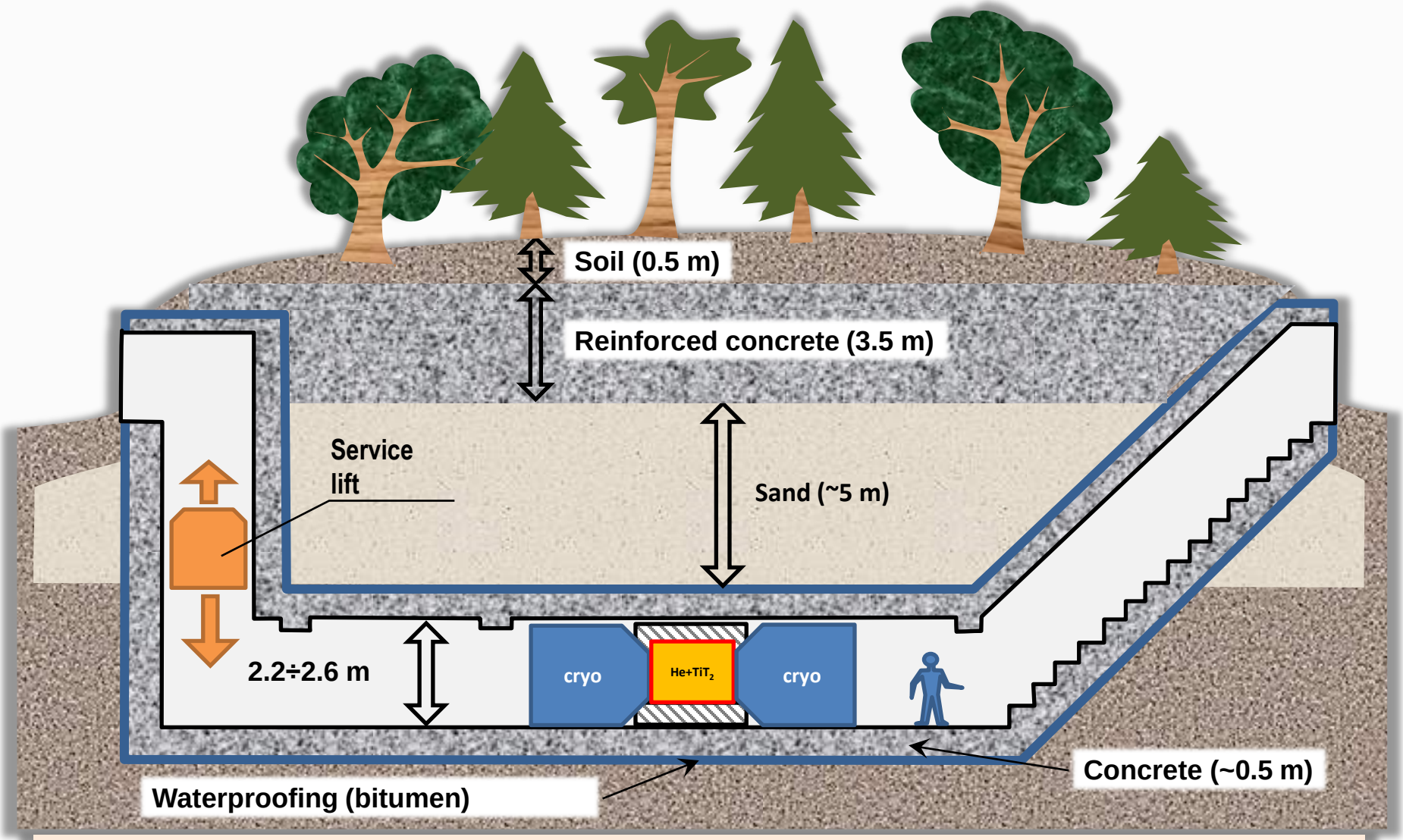

The overburden of ~18 m.w.e. stops the soft and hadronic components of cosmic radiation but **is not enough to sufficiently suppress the muon flux**

Discrimination of background events

General view of the cryostat

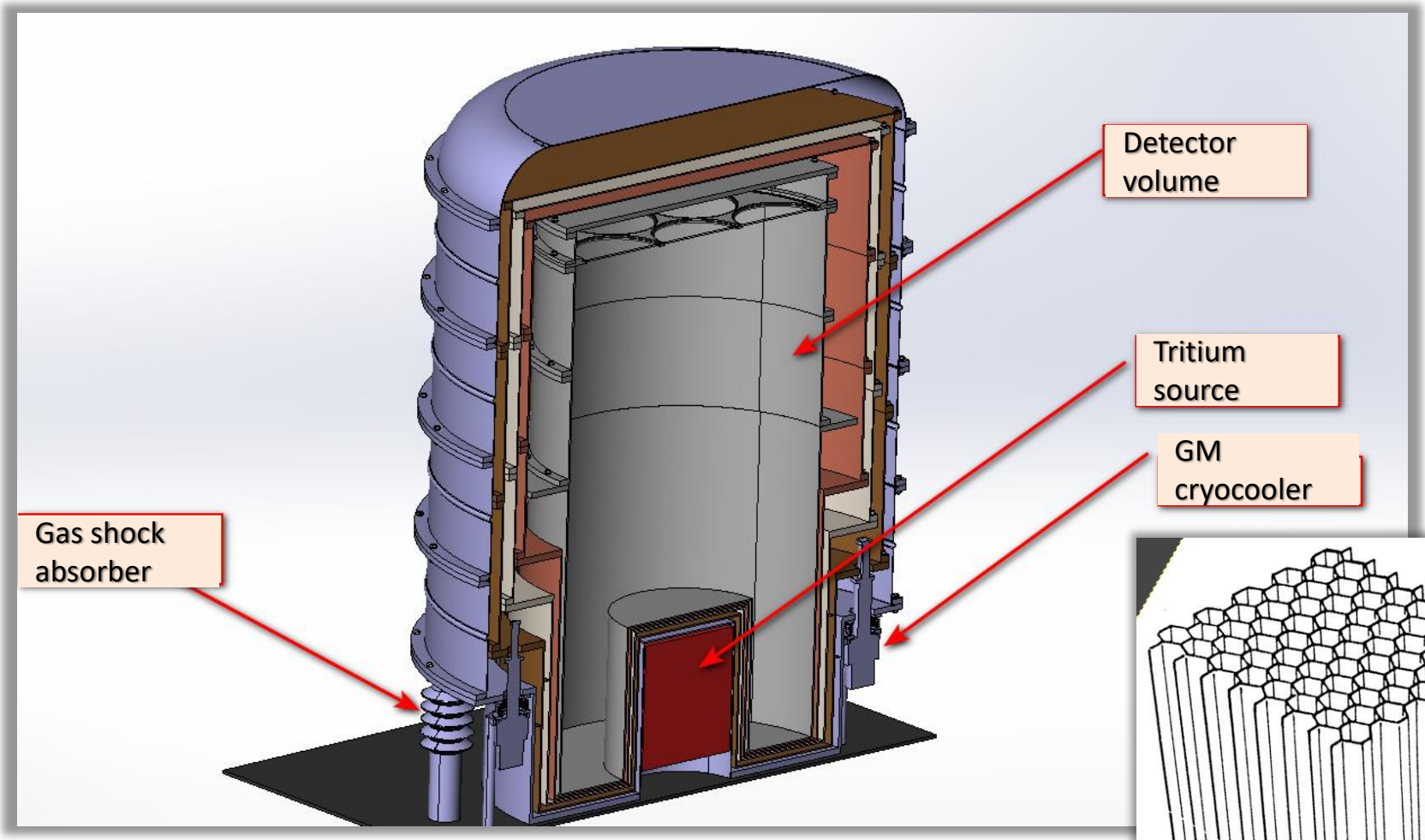

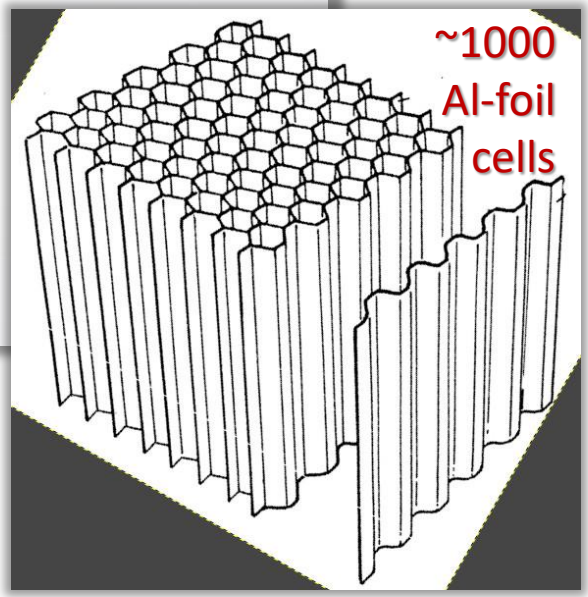

Segmentation of the He detector is the key to background discrimination

Atomic ionization channel

When the energy transfer T exceeds the maximal atomic recoil energy

$$T > T_R^{\max} = \frac{2E_\nu^2}{m}$$

the elastic neutrino-atom scattering channel is closed

Open channels:

$$\nu + \mathrm{X} \longrightarrow \mathrm{X}^* + \nu \qquad (T \geq \mathcal{E}_\mathrm{X}, \text{ excitation})$$

$$\nu + \mathrm{X} \longrightarrow \mathrm{X}^+ + e^- + \nu \qquad (T \geq I_\mathrm{X}, \text{ ionization})$$

$\mathcal{E}_\mathrm{X}$ and I_X are atomic excitation and ionization energies

World leading laboratory constraints on μ_ν, like those from XENNONnT and GEMMA, are obtained by studying the atomic ionization channel

Ionization cross section for tritium $\bar{\nu}_e$ on Si

SM predicts a flat spectrum at small T, and the μ_ν contribution $\propto \frac{1}{T}$

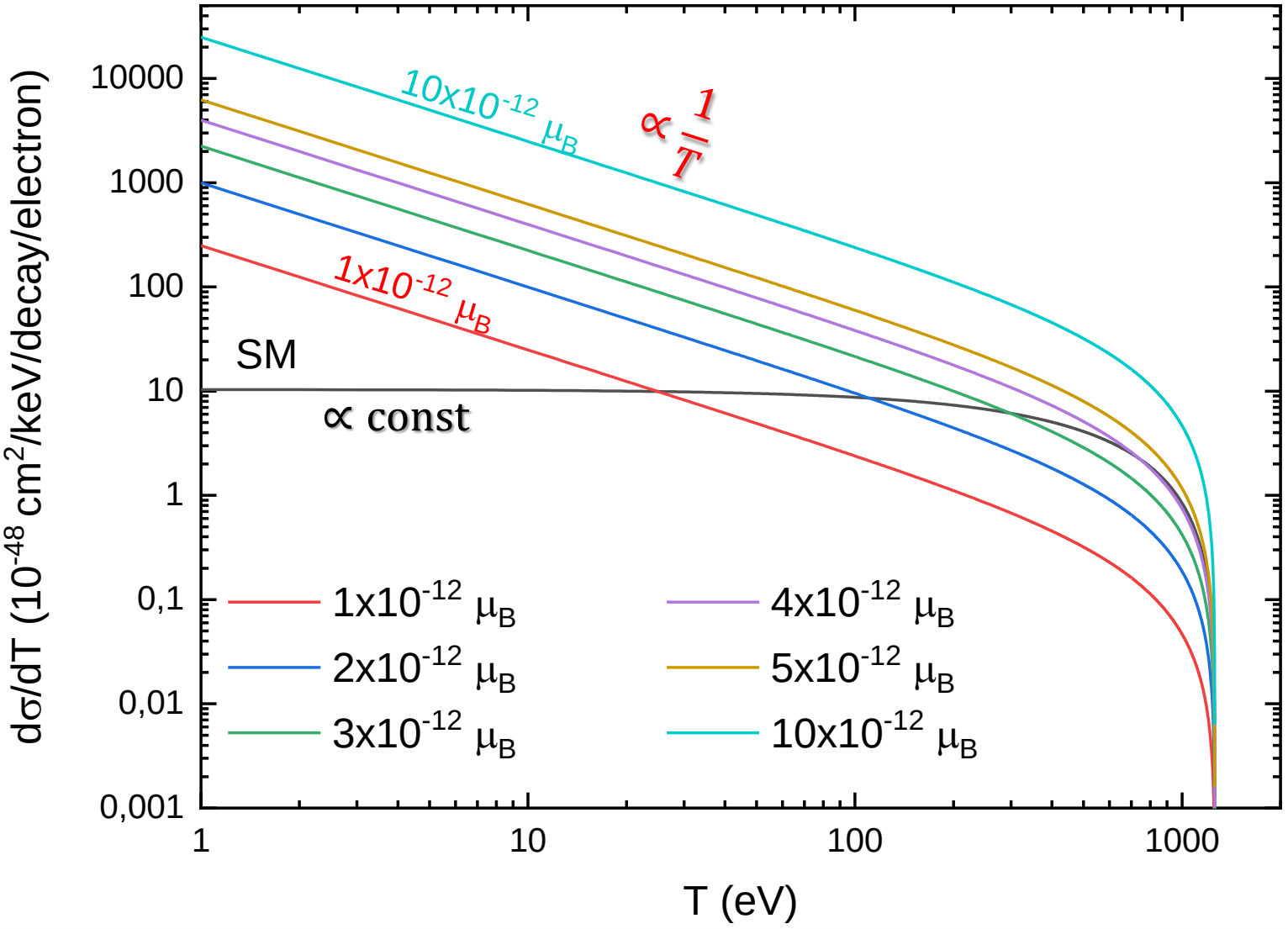

The detector's energy threshold needs to be as low as possible

Si detector concept

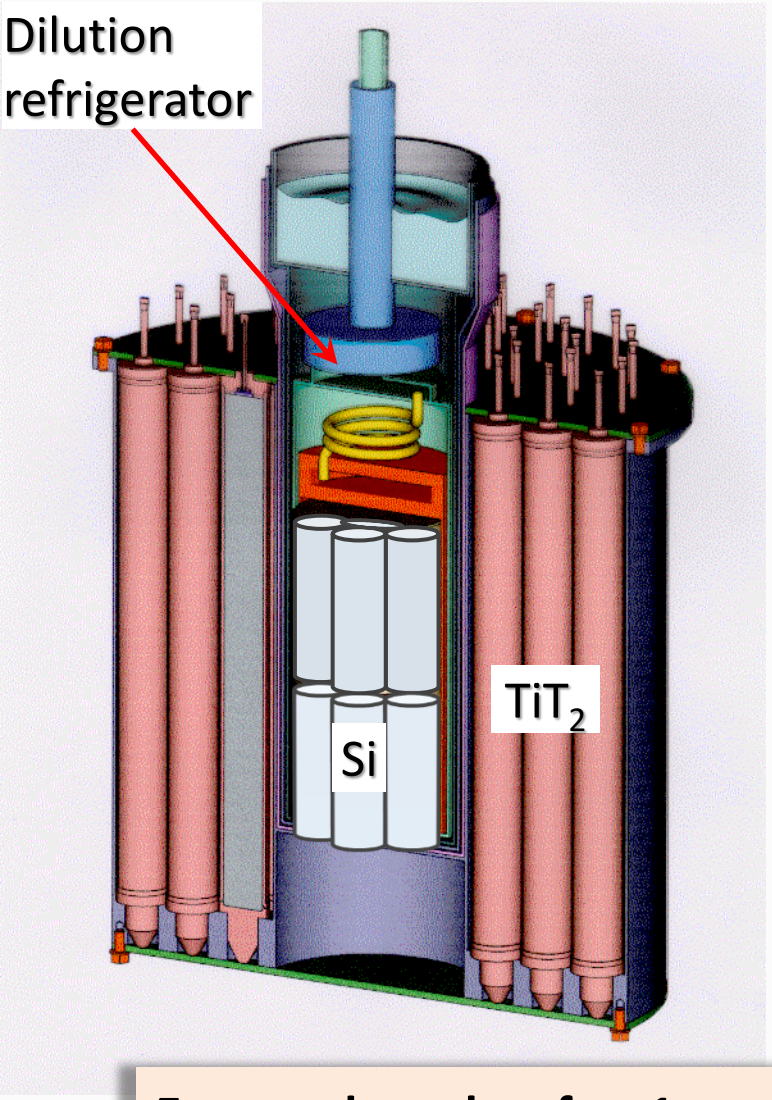

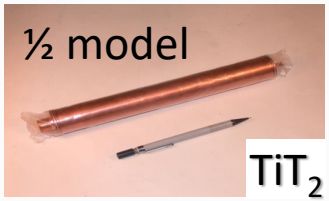

Tritium neutrino source (1-4 kg)

- tubular copper elements with TiT_2

Silicon cryodetectors (T=10-50 mK)
14×125 cm³, M=4 kg

- TES mounted on each Si crystal

The Si detector with an ultra-low threshold

E_{th}~10 eV or even E_{th} ~1 eV

owing to the Neganov-Trofimov-Luke effect

(heat amplification of ionization signal)

*B. Neganov and V. Trofimov, USSR patent no. 1037771, Otkrytia i Izobreteniya **146** (1985) 215;*

*P. N. Luke, J. Appl. Phys. **64** (1988) 6858.*

Expected results after 1 year of data collection

Number of events within SM: **~30 for 1 kg of T_2** and **~120 for 4 kg of T_2**

Sensitivity to neutrino magnetic moment: μ_ν**~(1-1.5)x10^{-12} μ_B** at 90% C.L.

CsI(pure) scintillation detector concept

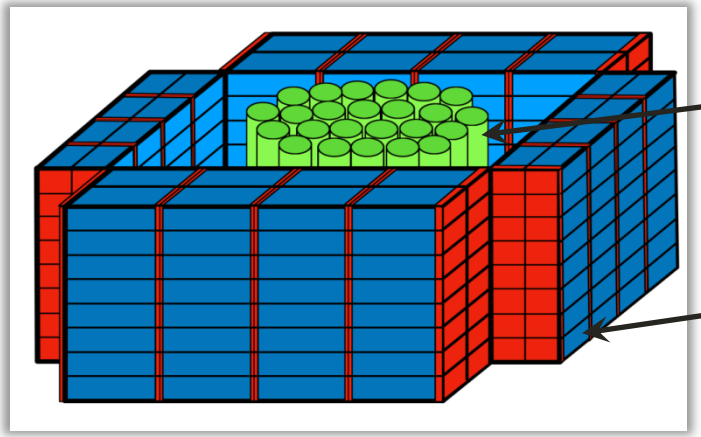

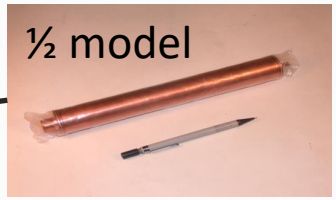

Tritium neutrino source (1-4 kg)

Tubular copper elements with TiT_2

15x15x50 mm³ CsI(pure) crystals at T=77 K, total mass is M=100 kg

- SiPM readout (two SiPMs per each crystal)
- Light collection at a level of 50 photoelectrons/keV
- Energy threshold is E_{th}~100 eV

*Abdurashitov, Vlasenko, Ivashkin, Silaeva, Sinev, Phys. Atom. Nuclei **85** (2022) 701*

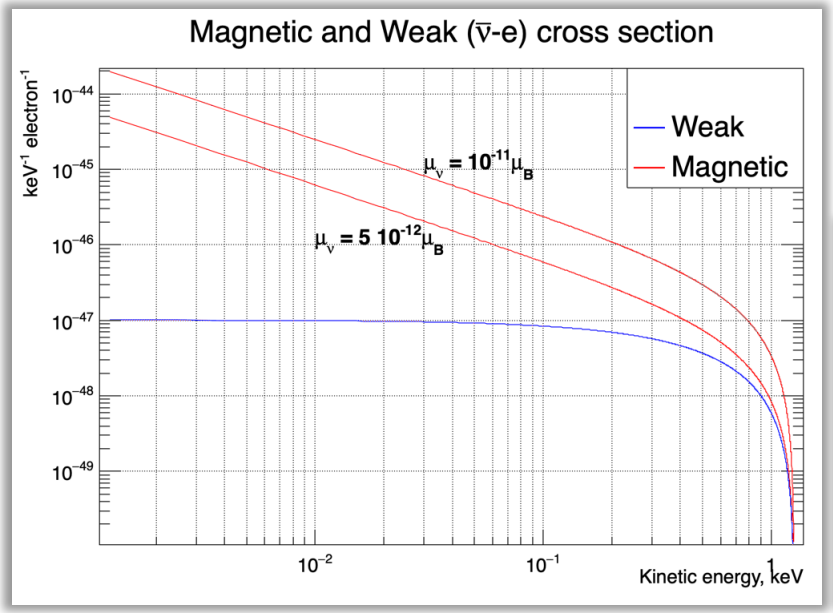

Expected results after 1 year of data collection

Number of events within SM:

~50 for 1 kg of T_2 and **~200 for 4 kg of T_2**

Sensitivity to neutrino magnetic moment:

μ_ν~(4-5)x10^{-12} μ_B

Summary and outlook

The Sarov tritium neutrino experiment aims at

(i) first observation of **coherent elastic neutrino-atom scattering** to test SM neutrino interactions at unprecedentedly low energies

(ii) search for **neutrino magnetic moment**

A high-intensity tritium neutrino source is being prepared

- at least **1 kg, 10 MCi** (possibly up to **4 kg, 40 MCi**)

A 1000-L He II detector is being developed (to be **ready by 2027**)

- observation of **CEνAS (2032)**
- sensitivity to μ_ν **~ (2-4)x10^{-13} μ_B (2032)**

A 4-kg Si detector is being developed (to be **ready by 2026**)

- sensitivity to μ_ν **~ (1-1.5)x10^{-12} μ_B (2027)**

A 100-kg CsI detector is being developed (to be **ready by 2025**)

- sensitivity to μ_ν **~ (4-5)x10^{-12} μ_B (2026)**

Collaboration

National Center
FOR PHYSICS AND MATHEMATICS

RUSSIAN FEDERAL NUCLEAR CENTER
ALL-RUSSIAN RESEARCH INSTITUTE OF EXPERIMENTAL PHYSICS

PRODUCTION
ASSOCIATION
MAYAK

NIZHNY NOVGOROD STATE
TECHNICAL UNIVERSITY
N.A. R.E. ALEKSEEV

LOMONOSOV MOSCOW
STATE UNIVERSITY

LOBACHEVSKY
UNIVERSITY

JOINT INSTITUTE
FOR NUCLEAR RESEARCH

IPM RAS

Ioffe
Physical-
Technical
Institute

Progress of experimental sensitivity to μ_ν

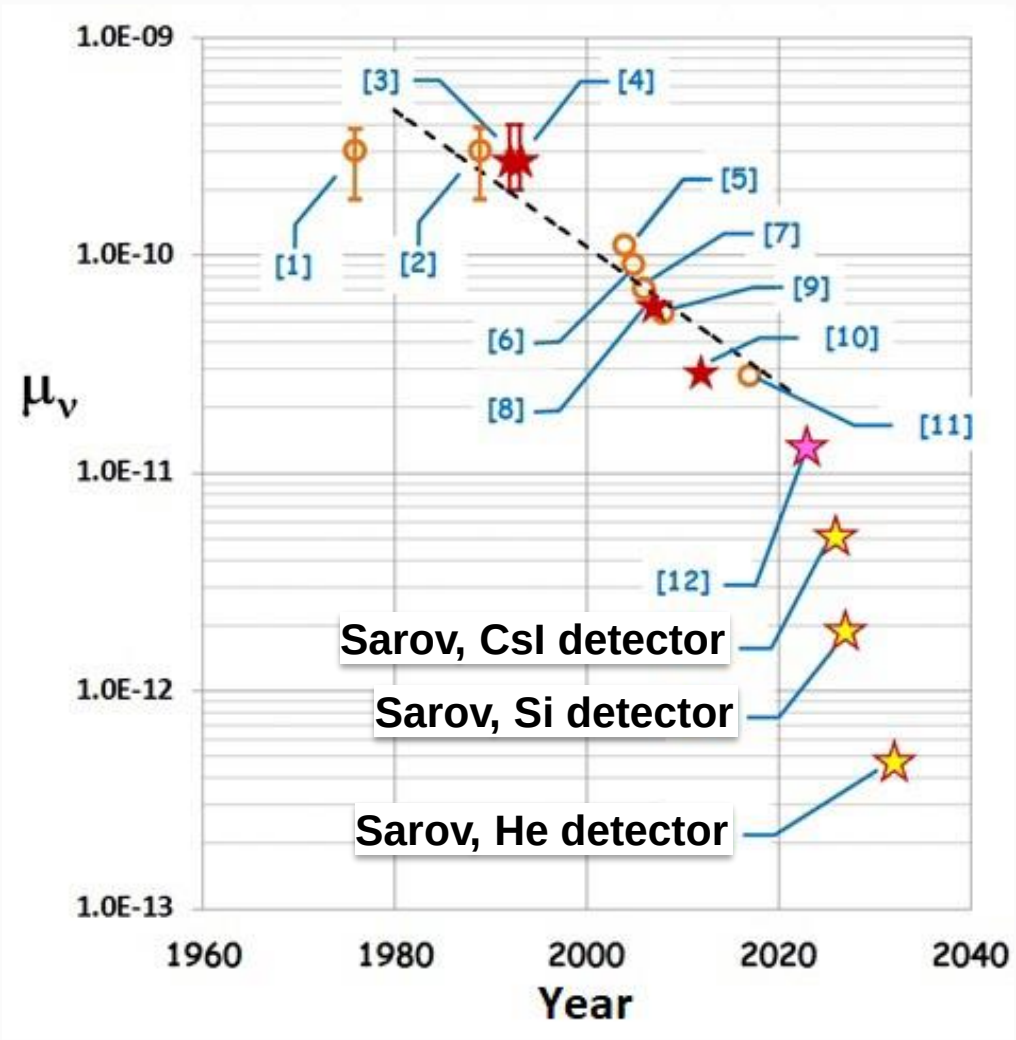

Please see our poster

O. Moskalev et al.

Status and prospects of implementation of the Sarov tritium neutrino experiment

Thank you for your attention!

Backup slides

Coherent elastic neutrino-nucleus scattering

Experiment COHERENT (SNS, Oak Ridge, Tennessee)

Science REPORTS

Cite as: D. Akimov *et al.*, *Science* 10.1126/science.aao0990 (2017).

Observation of coherent elastic neutrino-nucleus scattering

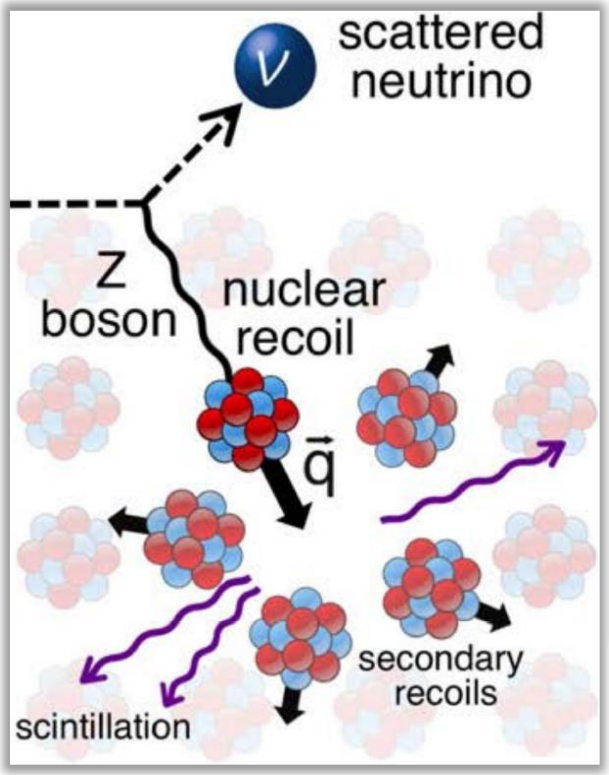

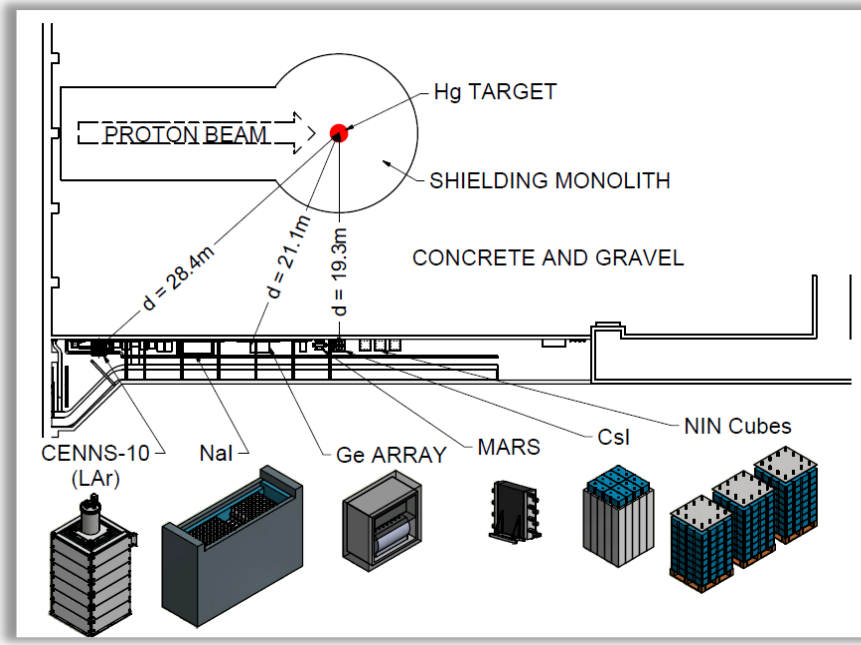

14.6 kg CsI scintillating crystal

Why CEνNS?

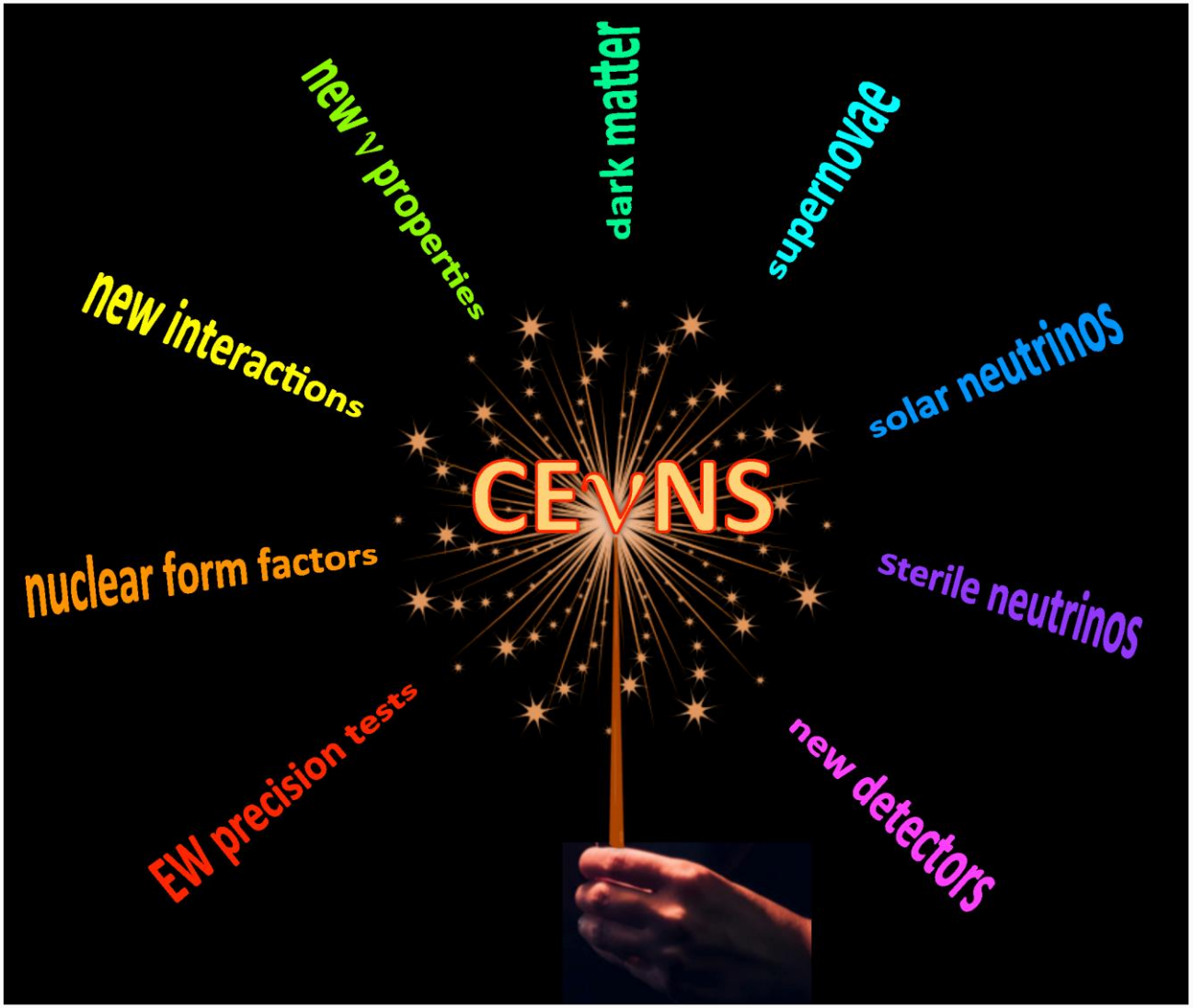

[E. Lisi, Neutrino 2018]

Coherent elastic neutrino-atom scattering

Elastic neutrino-atom scattering in SM

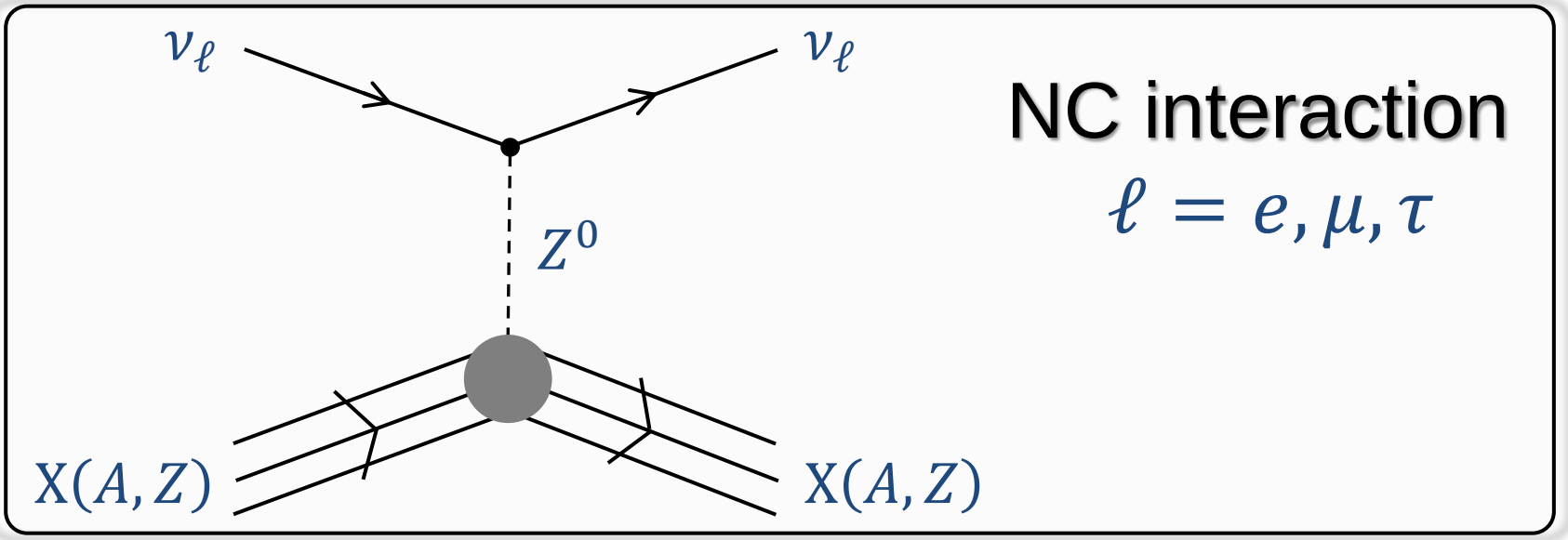

NC interaction

$\ell = e, \mu, \tau$

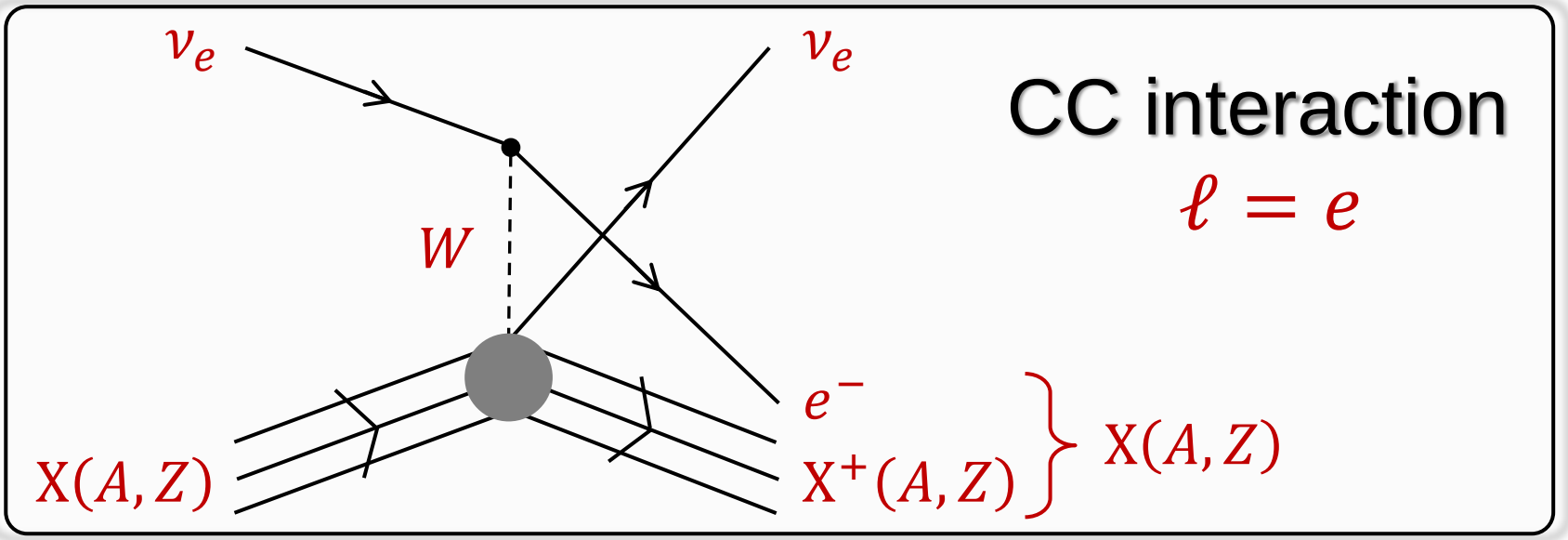

CC interaction

$\ell = e$

CEνAS cross section in SM

$$d\sigma = \frac{(2\pi)^4}{4E_\nu m}\delta^4(p+k-p'-k')\left|\mathcal{M}^{(\mathrm{SM})}\right|^2 \frac{d^3p'_\nu}{(2\pi)^3 2E'_\nu}\frac{d^3k'}{(2\pi)^3 2E'}$$

$$p=(E_\nu,\mathbf{p}_\nu), \qquad p'=(E'_\nu,\mathbf{p}'_\nu), \qquad k=(m,0), \qquad k'=(E',\mathbf{k}')$$

$$\mathcal{M}^{(\mathrm{SM})} = \frac{G_F}{\sqrt{2}} j^\lambda J_\lambda, \qquad j^\lambda = \bar{u}_\nu(p')\gamma^\lambda(1-\gamma^5)u_\nu(p), \qquad J^\lambda = J_p^\lambda + J_n^\lambda + J_e^\lambda$$

The proton, neutron and electron currents:

$$J_p^\lambda = \left\langle i\left|\sum_{j=1}^{Z} e^{i\mathbf{q}\mathbf{r}_j^{(p)}}\gamma_j^0\gamma_j^\lambda\left(g_V^{(p)}-\frac{1}{2}g_A^{(p)}\gamma_j^5\right)\right|i\right\rangle, \quad g_V^{(p)}=\frac{1}{2}-2\sin^2\theta_W\,, \quad g_A^{(p)}=1.25$$

$$J_n^\lambda = \left\langle i\left|\sum_{j=1}^{N} e^{i\mathbf{q}\mathbf{r}_j^{(n)}}\gamma_j^0\gamma_j^\lambda\left(g_V^{(n)}-\frac{1}{2}g_A^{(n)}\gamma_j^5\right)\right|i\right\rangle, \quad g_V^{(n)}=-\frac{1}{2}, \quad g_A^{(n)}=-1.25$$

$$J_e^\lambda = \left\langle i\left|\sum_{j=1}^{Z} e^{i\mathbf{q}\mathbf{r}_j^{(e)}}\gamma_j^0\gamma_j^\lambda\left(g_V^{(e)}-g_A^{(e)}\gamma_j^5\right)\right|i\right\rangle,$$

$$g_V^{(e)} = 2\sin^2\theta_W - \frac{1}{2} + \delta_{\ell e}, \qquad g_A^{(e)} = -\frac{1}{2} + \delta_{\ell e}$$

Customary approximations

i. Neglecting hyperfine coupling: $|i\rangle = |\Psi_{\text{nuc}}\rangle \times |\Psi_{\text{el}}\rangle$

ii. Treating the currents nonrelativistically:

$$J_p^0 = g_V^{(p)} \left\langle \Psi_{\text{nuc}} \left| \sum_{j=1}^{Z} e^{i\mathbf{q}\mathbf{r}_j^{(p)}} \right| \Psi_{\text{nuc}} \right\rangle = g_V^{(p)} Z F_{\text{nuc}}(q^2)$$

$$J_n^0 = g_V^{(n)} \left\langle \Psi_{\text{nuc}} \left| \sum_{j=1}^{N} e^{i\mathbf{q}\mathbf{r}_j^{(n)}} \right| \Psi_{\text{nuc}} \right\rangle = g_V^{(n)} N F_{\text{nuc}}(q^2)$$

$$J_p^3 = \frac{1}{2} g_A^{(p)} \left\langle \Psi_{\text{nuc}} \left| \sum_{j=1}^{Z} e^{i\mathbf{q}\mathbf{r}_j^{(p)}} \hat{\sigma}_j^3 \right| \Psi_{\text{nuc}} \right\rangle = \frac{1}{2} g_A^{(p)} (Z_+ - Z_-) F_{\text{nuc}}(q^2)$$

$$J_n^3 = \frac{1}{2} g_A^{(n)} \left\langle \Psi_{\text{nuc}} \left| \sum_{j=1}^{Z} e^{i\mathbf{q}\mathbf{r}_j^{(n)}} \hat{\sigma}_j^3 \right| \Psi_{\text{nuc}} \right\rangle = \frac{1}{2} g_A^{(n)} (N_+ - N_-) F_{\text{nuc}}(q^2)$$

$$J_e^0 = g_V^{(e)} \left\langle \Psi_{\text{el}} \left| \sum_{j=1}^{Z} e^{i\mathbf{q}\mathbf{r}_j^{(e)}} \right| \Psi_{\text{el}} \right\rangle = g_V^{(e)} Z F_{\text{el}}(q^2)$$

$$J_e^3 = g_A^{(e)} \left\langle \Psi_{\text{el}} \left| \sum_{j=1}^{Z} e^{i\mathbf{q}\mathbf{r}_j^{(e)}} \hat{\sigma}_j^3 \right| \Psi_{\text{el}} \right\rangle = g_A^{(e)} F_{\text{el}}^3(q^2)$$

$$F_{\text{nuc}}(q^2) = \frac{1}{A} \int d^3r e^{i\mathbf{q}\mathbf{r}} \rho_{\text{nuc}}(\mathbf{r}), \qquad F_{\text{el}}(q^2) = \frac{1}{Z} \int d^3r e^{i\mathbf{q}\mathbf{r}} \rho_{\text{el}}(\mathbf{r})$$

$$F_{\text{el}}^3(q^2) = \frac{1}{Z} \int d^3r e^{i\mathbf{q}\mathbf{r}} \left\langle \Psi_{\text{el}} \left| \sum_{j=1}^{Z} \delta\left(\mathbf{r} - \mathbf{r}_j^{(e)}\right) \hat{\sigma}_j^3 \right| \Psi_{\text{el}} \right\rangle$$

CEνAS cross section in SM

Yu. V. Gaponov and V. N. Tikhonov, Yad. Fiz. (USSR) ***26****, 594 (1977);*
L. M. Sehgal and M. Wanninger, Phys. Lett. B ***171****, 107 (1986)*

$$\frac{d\sigma}{dT} = \frac{G_F^2 m}{\pi}\left[C_V^2\left(1-\frac{mT}{2E_\nu^2}\right)+C_A^2\left(1+\frac{mT}{2E_\nu^2}\right)\right]$$

$$C_V = \left[Z\left(\tfrac{1}{2}-2\sin^2\theta_W\right)-\tfrac{1}{2}N\right]F_{\rm nuc}(q^2)+Z\left(\mp\tfrac{1}{2}+2\sin^2\theta_W\right)F_{\rm el}(q^2)$$

$$C_A^2 = (C_A^{\rm nuc})^2+\tfrac{1}{4}\sum_{n,l}\left[\left(L_+^{nl}-L_-^{nl}\right)F_{\rm el}^{nl}(q^2)\right]^2$$

$$C_A^{\rm nuc} = \tfrac{g_A}{2}\left[(Z_+-Z_-)-(N_+-N_-)\right]F_{\rm nuc}(q^2), \qquad g_A = 1.25$$

plus (minus) stands for $\nu=\nu_e$ ($\nu=\nu_{\mu,\tau}$)

q is the momentum transfer, with $q^2 = 2mT$

$F_{\rm nuc(el)}(q^2)$ is the Fourier transform of the nuclear (electron) density.

Z (N) is the number of protons (neutrons)

$Z_\pm$ and $N_\pm$ ($L_\pm^{nl}$) are the numbers of protons and neutrons (electrons) with spin parallel (+) or antiparallel (−) to the nucleus spin (the total electron spin)


Neutrino electromagnetic
properties in CEνAS

Unsolved problems in neutrino physics

- Neutrino mass ($m_\nu = ?$) and mass hierarchy (NO or IO)
- CP violation in neutrino oscillations
- Dirac ($\nu \neq \bar{\nu}$) or Majorana ($\nu = \bar{\nu}$)
- Number of neutrino types:

  $N_\nu = 3$ or $N_\nu > 3$
- Neutrino nonstandard interactions
- **Neutrino electromagnetic properties**

Neutrino electromagnetic properties

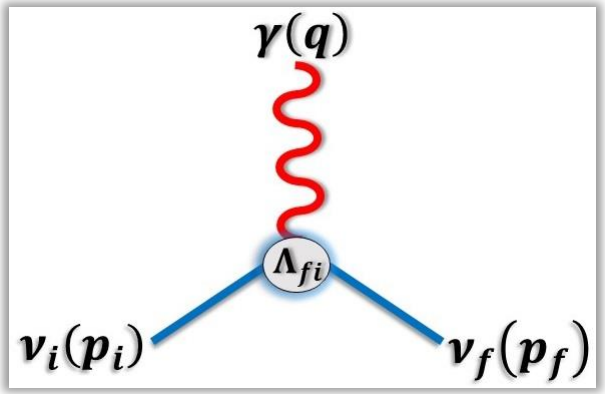

C. Giunti and A. Studenikin, Neutrino electromagnetic interactions: A window to new physics, Rev. Mod. Phys. ***87*** *(2015) 531; arXiv:1403.6344*

The effective neutrino electromagnetic vertex (under the Lorentz and gauge invariance):

$$\Lambda_{\mu}^{(\mathrm{EM};\nu)fi}(q) = \left(\gamma_\mu - \frac{q_\mu q}{q^2}\right)\left[f_Q^{fi}(q^2) - q^2 f_A^{fi}(q^2)\gamma_5\right] - i\sigma_{\mu\nu}q^\nu\left[f_M^{fi}(q^2) + i f_E^{fi}(q^2)\gamma_5\right]$$

$f_{Q,A,M,E}^{fi}$ are charge (Q), anapole (A), magnetic (M) and electric (E) form factors of diagonal ($i = f$) and transition ($i \neq f$) types.

$f_Q^{fi}(0) = e_{fi}$, where e_{fi} is millicharge,
$f_A^{fi}(0) = a_{fi}$, where a_{fi} is anapole moment,
$f_M^{fi}(0) = \mu_{fi}$, where μ_{fi} is magnetic moment,
$f_E^{fi}(0) = \epsilon_{fi}$, where ϵ_{fi} is electric dipole moment

$q^2 \to 0$: $f_Q^{fi}(q^2) = e_{fi} + \frac{1}{6}\langle r_\nu^2\rangle_{fi} q^2$, where $\langle r_\nu^2\rangle_{fi}$ is the neutrino charge radius.

Neutrino magnetic moment

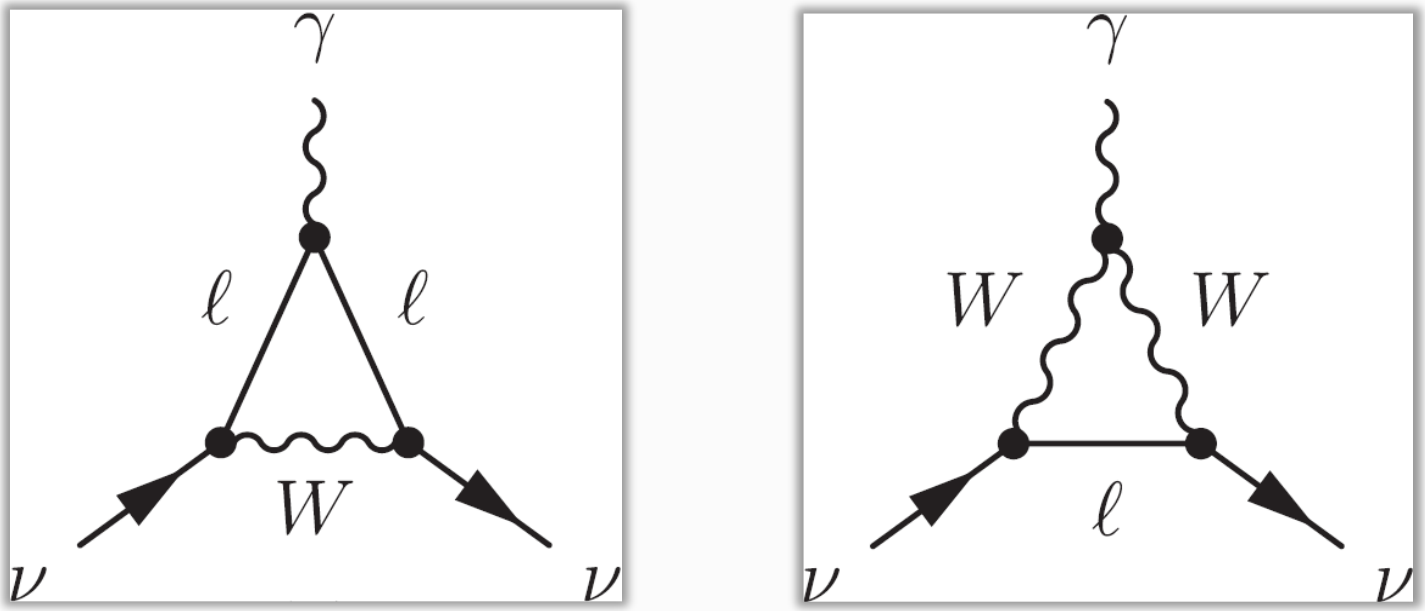

K. Fujikawa and R. Shrock, Phys. Rev. Lett. ***45*** *(1980) 963*

In the minimally extended SM with addition of right-handed massive Dirac neutrinos:

$$\mu_\nu \simeq 3.2 \times 10^{-19} \mu_B \left(\frac{m_\nu}{1\ \text{eV}}\right)$$

$m_\nu < 0.8$ eV at 90% CL

M. Aker et al. (The KATRIN Collaboration), Nature Physics ***18*** *(2022) 160*

Ionizing neutrino-atom interactions

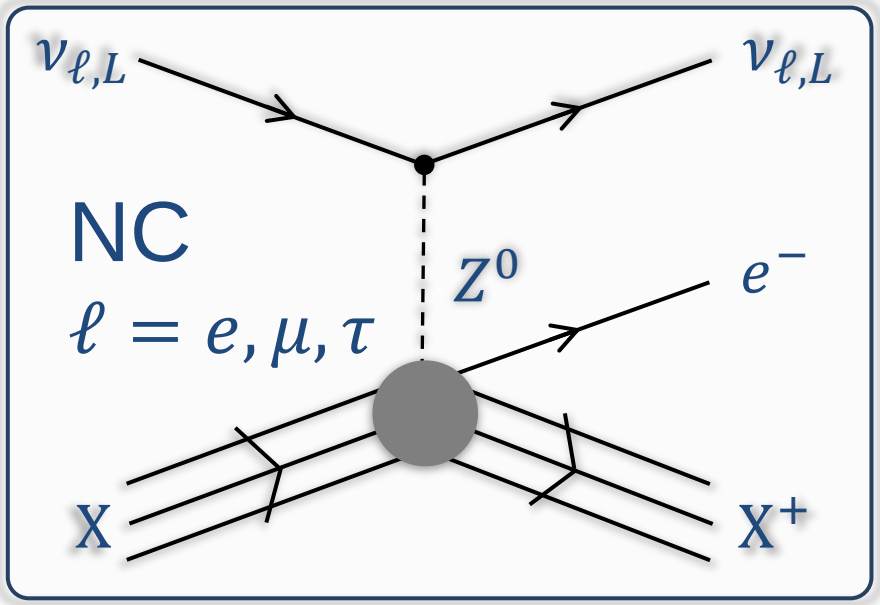

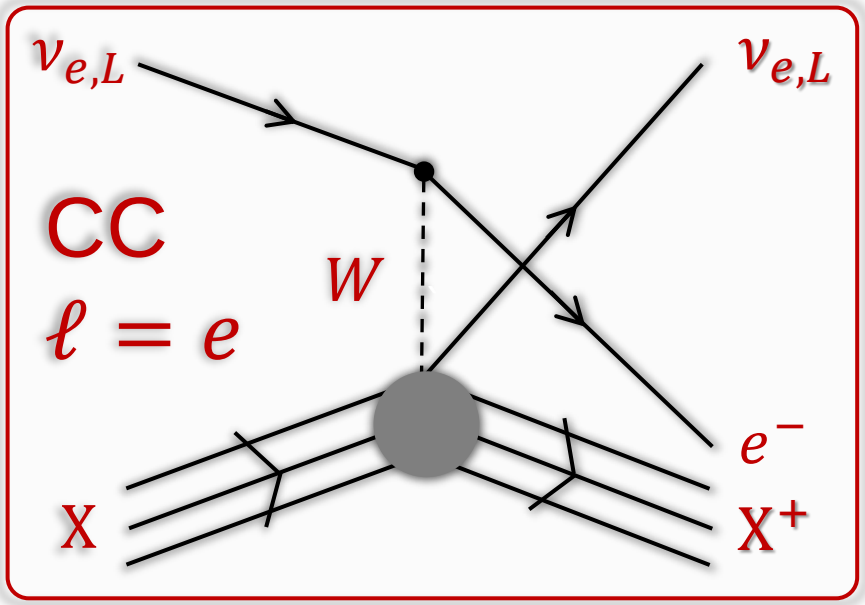

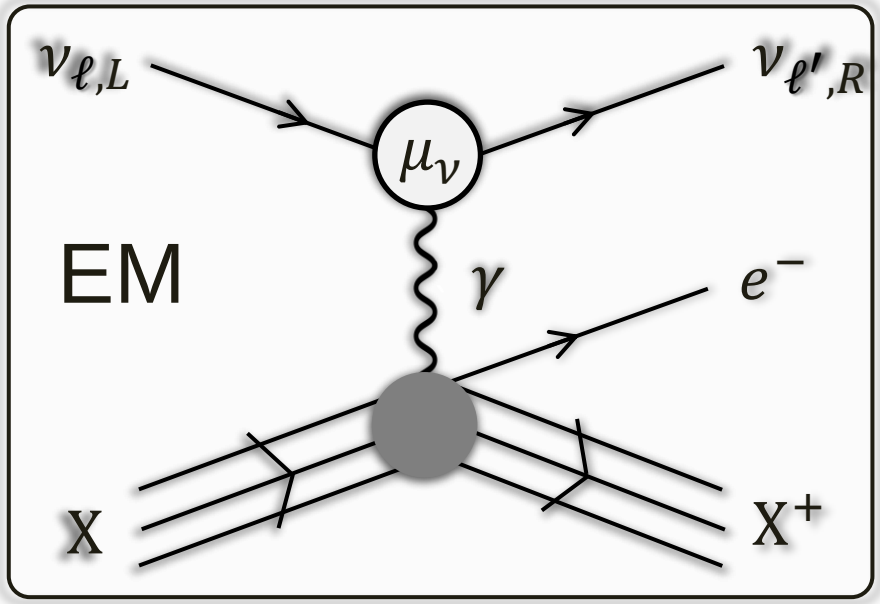

Unlike the SM weak NC and CC interactions, the μ_ν interaction flips the neutrino helicity ($L \rightarrow R$) and can change the neutrino flavor if the transition magnetic moment ($\ell \neq \ell'$) is nonzero.

XENON1T anomaly

E. Aprile et al. (XENON Collaboration), Phys. Rev. D **102** (2020) 072004

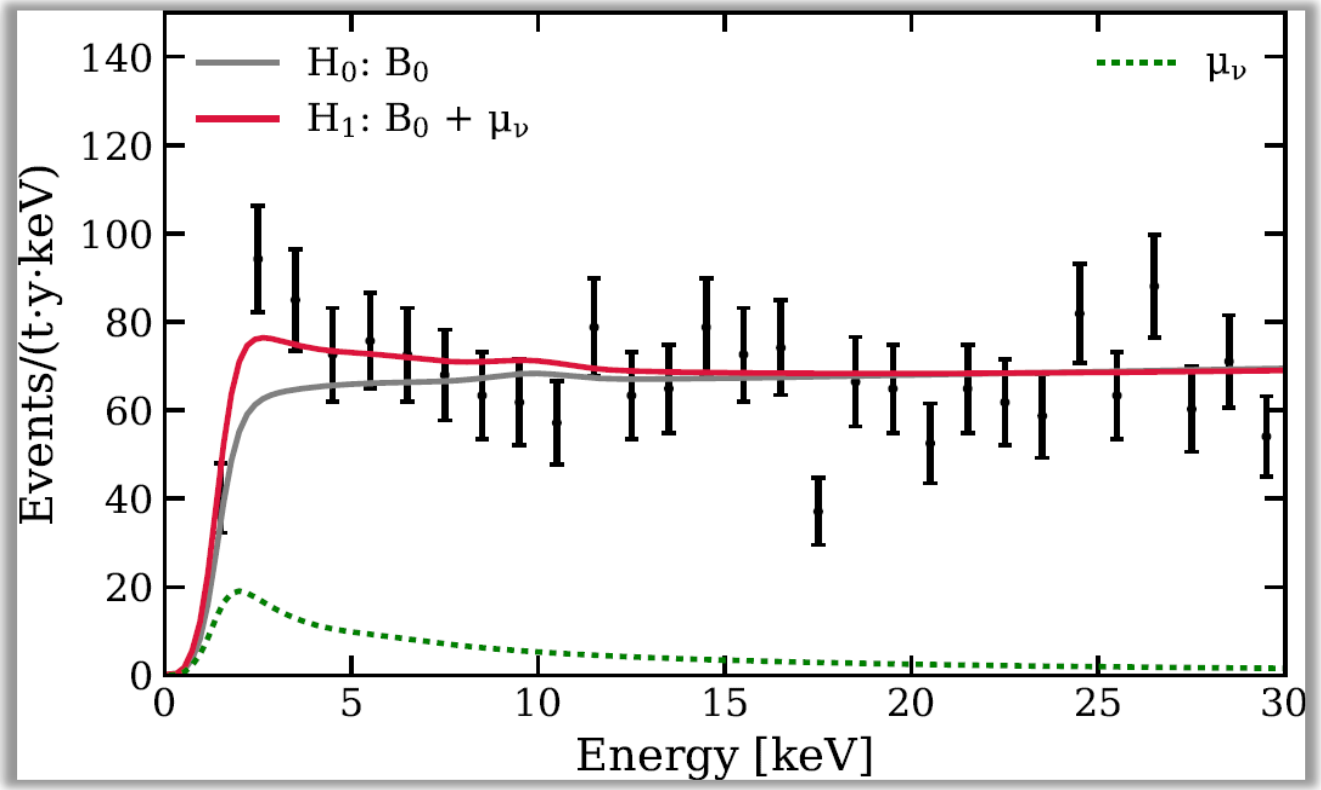

Grey solid curve ($H_0 : B_0$) is the standard background model for the electron recoil in a 3.2-ton liquid Xe detector.

Red solid curve ($H_1 : B_0 + \mu_\nu$) accounts for the solar neutrino magnetic moment from the 90% confidence interval $\mu_\nu \in (1.4, 2.9) \times 10^{-11} \mu_B$.

Green dashed curve (μ_ν) shows the magnetic moment contribution.

Electromagnetic interactions in CEνAS

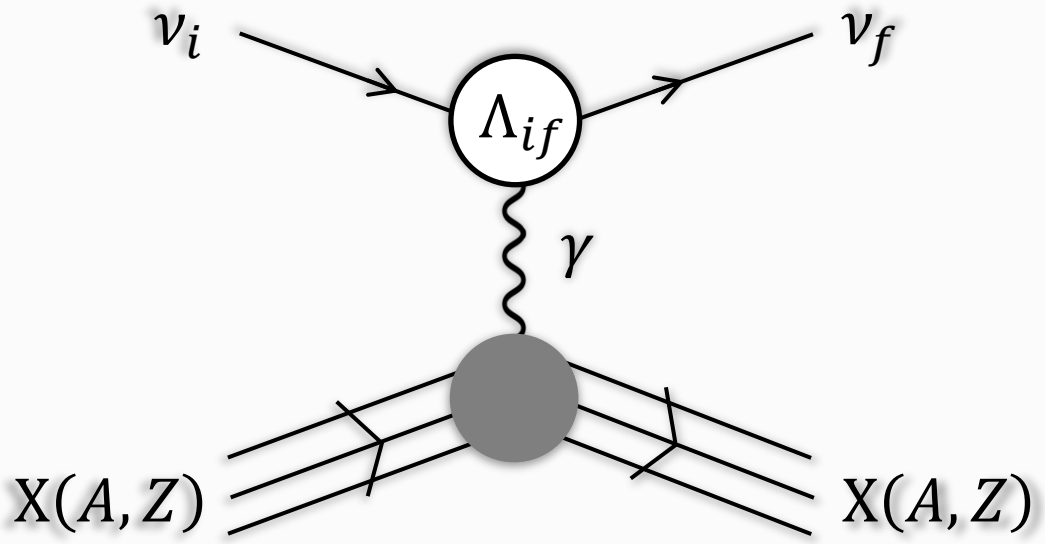

$$\Lambda_{\mu}^{(\mathrm{EM};\nu)fi}(q) = \left(\gamma_\mu - \frac{q_\mu q}{q^2}\right)\left[f_Q^{fi}(q^2) - q^2 f_A^{fi}(q^2)\gamma_5\right] - i\sigma_{\mu\nu}q^\nu\left[f_M^{fi}(q^2) + if_E^{fi}(q^2)\gamma_5\right]$$

$$\sigma_{\mu\nu} = \frac{i}{2}(\gamma_\mu\gamma_\nu - \gamma_\nu\gamma_\mu)$$

$q^2 \to 0$: $f_Q(q^2) - q^2 f_A(q^2)\gamma_5 = e_\nu + \frac{q^2}{6}(\langle r_\nu^2\rangle - 6a_\nu\gamma_5)$

$f_M(q^2) + if_E(q^2)\gamma_5 = \mu_\nu + \mathrm{i}\epsilon_\nu\gamma_5$

$\gamma_5 = -1$ for ν and $\gamma_5 = +1$ for $\bar{\nu}$

EM contribution to CEνAS cross section

$$d\sigma = \frac{(2\pi)^4}{4E_\nu m}\delta^4(p+k-p'-k')\sum_{\ell'}\left|\mathcal{M}_{\nu_\ell\to\nu_{\ell'}}\right|^2\frac{d^3p'_\nu}{(2\pi)^3 2E'_\nu}\frac{d^3k'}{(2\pi)^3 2E'}$$

$$p=(E_\nu,\mathbf{p}_\nu),\ p'=(E'_\nu,\mathbf{p}'_\nu),\qquad k=(m,0),\ k'=(E',\mathbf{k}'),\qquad q=p-p'$$

$$\mathcal{M}_{\nu_\ell\to\nu_{\ell'}}=\delta_{\ell\ell'}\mathcal{M}^{(\mathrm{SM})}+\mathcal{M}^{(\mathrm{EM})},\qquad \mathcal{M}^{(\mathrm{EM})}=\mathcal{M}^{(e_\nu)}+\mathcal{M}^{(\mu_\nu)},$$

$$\mathcal{M}^{(e_\nu)}=-\frac{4\pi\alpha}{q^2}\bar{u}_{\nu_{\ell'}}(p')\gamma_\lambda\left[e_\nu+\frac{q^2}{6}(\langle r_\nu^2\rangle-6a_\nu\gamma_5)\right]u_{\nu_\ell}(p)\left[J^\lambda_{V,p}(q)-J^\lambda_{V,e}(q)\right]$$

$$\mathcal{M}^{(\mu_\nu)}=i\frac{2\pi\alpha}{m_e q^2}\bar{u}_{\nu_{\ell'}}(p')\sigma_{\lambda\rho}q^\rho(\mu_\nu+\mathrm{i}\epsilon_\nu\gamma_5)u_{\nu_\ell}(p)\left[J^\lambda_{V,p}(q)-J^\lambda_{V,e}(q)\right]$$

The proton and electron vector currents:

$$J^\lambda_{V,p}(q)=\left\langle i\left|\sum_{j=1}^{Z}e^{i\mathbf{q}\mathbf{r}_j^{(p)}}\gamma_j^0\gamma_j^\lambda\right|i\right\rangle,\qquad J^\lambda_{V,e}(q)=\left\langle i\left|\sum_{j=1}^{Z}e^{i\mathbf{q}\mathbf{r}_j^{(e)}}\gamma_j^0\gamma_j^\lambda\right|i\right\rangle$$

The e_ν and μ_ν effects in CEνAS

$$\frac{d\sigma}{dT} = \frac{d\sigma^{(\mathrm{SM};e_\nu)}}{dT} + \frac{d\sigma^{(\mu_\nu)}}{dT}$$

The e_ν effect (e_ν is in units of e):

$$\frac{d\sigma^{(\mathrm{SM};e_\nu)}}{dT} = \frac{G_F^2 m}{\pi}\left[C_V^2\left(1-\frac{mT}{2E_\nu^2}\right)+C_A^2\left(1+\frac{mT}{2E_\nu^2}\right)\right]$$

$$C_V = C_V^{\mathrm{SM}} + \frac{\sqrt{2}\pi\alpha Z e_\nu}{G_F m T}[1-F_{\mathrm{el}}(q^2)], \qquad q^2 = 2mT$$

The μ_ν effect (μ_ν is in units of μ_B):

$$\frac{d\sigma^{(\mu_\nu)}}{dT} = \frac{\pi\alpha^2 Z^2}{m_e^2}|\mu_\nu|^2\left(\frac{1}{T}-\frac{1}{E_\nu}\right)[1-F_{\mathrm{el}}(q^2)]^2$$

CEνAS cross sections for $\bar{\nu}_e$ with E_ν=10 keV

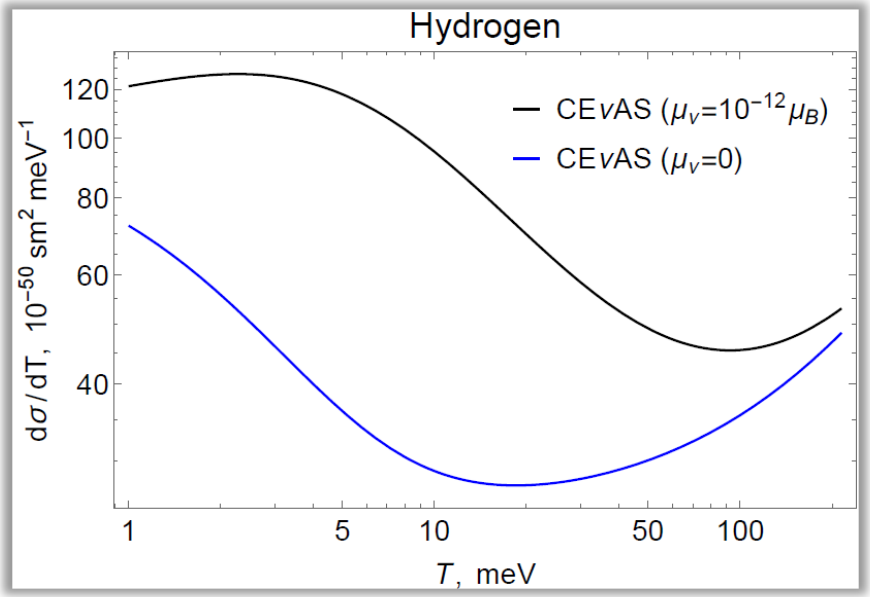

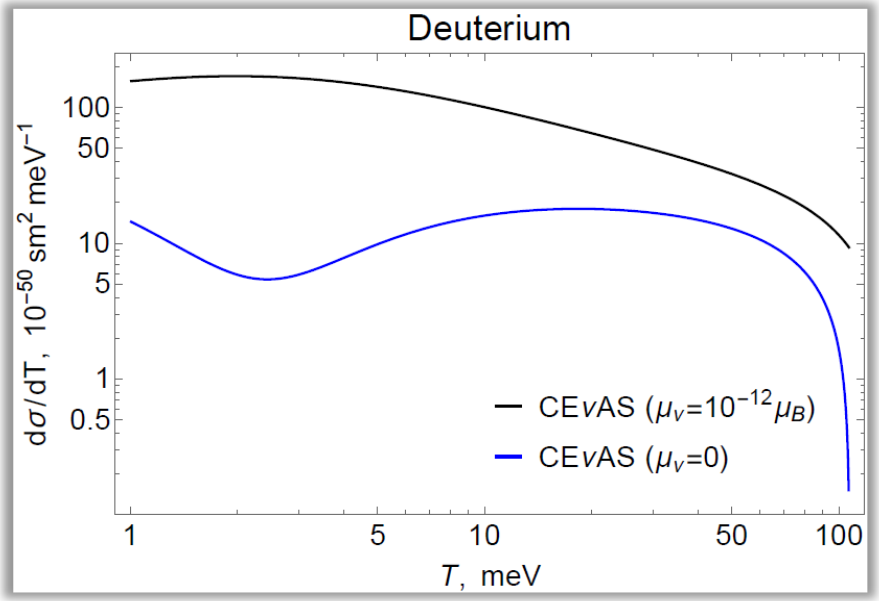

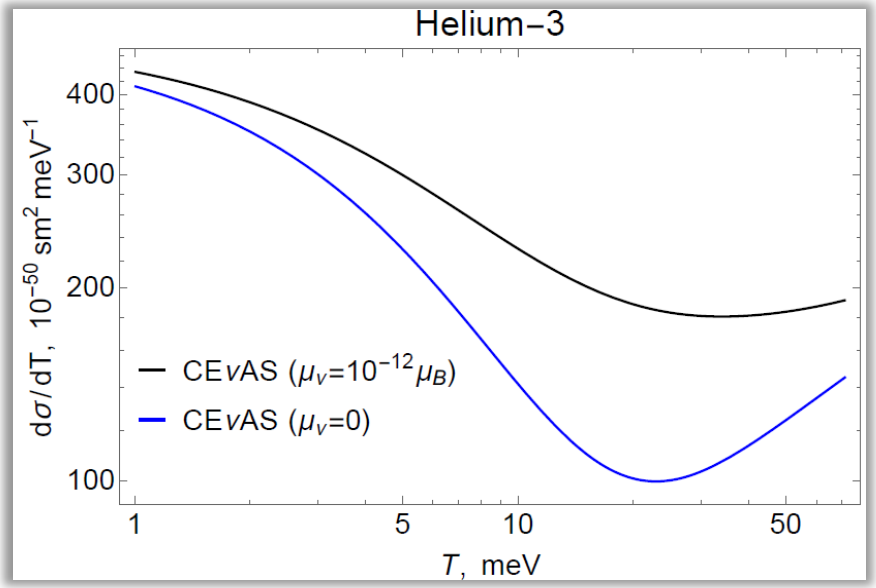

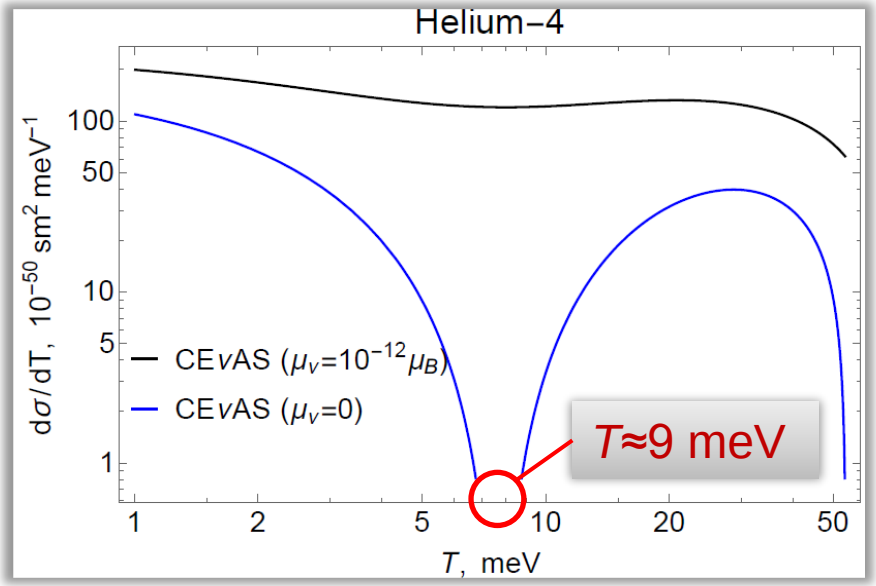

Donchenko, Kouzakov, Studenikin, JETP Lett. ***117****, 879 (2023)*


Detection methods

Detection method to study CEνAS

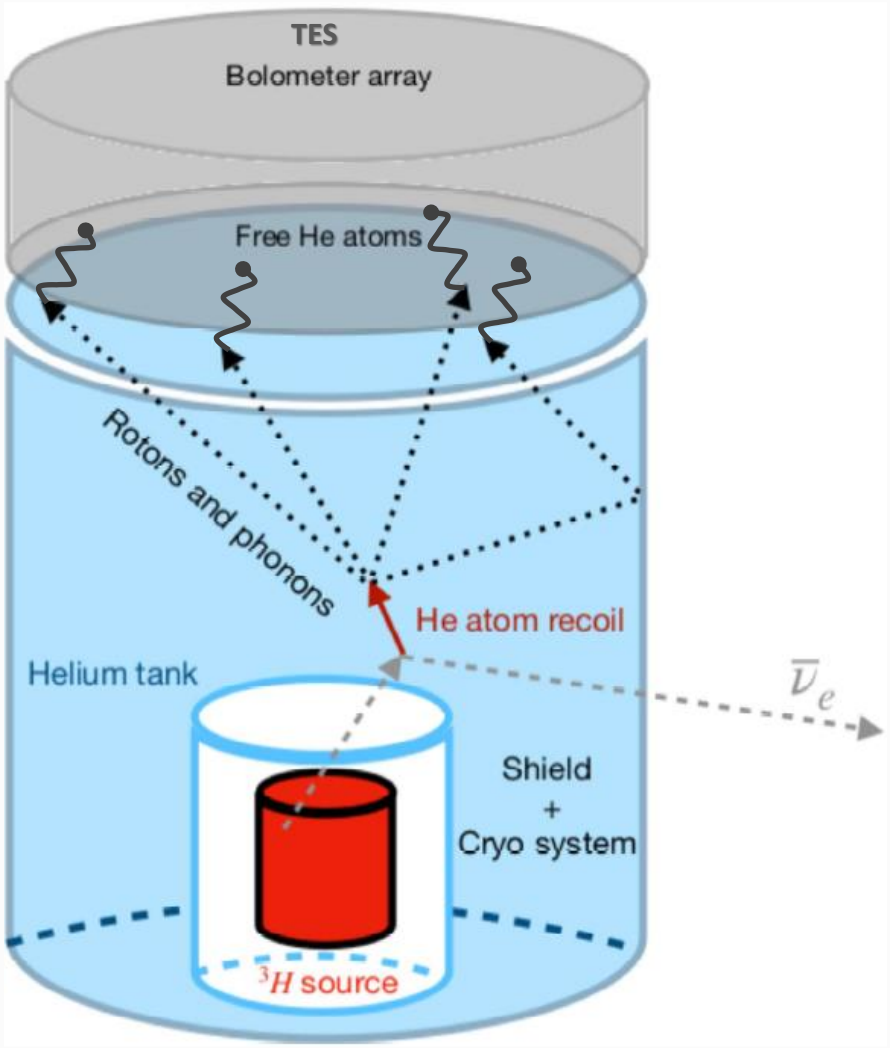

Tritium neutrino

↓

Elastic neutrino-atom scattering

↓

He atom recoil (1-185 meV)

↓

Phonons and rotons (0.7-1.2 meV per q. p.)

↓

Quantum evaporation (0.6 meV per atom)

↓

Adsorption onto TES (6-50 meV per adatom)

↓

Signal

Tritium neutrino source (TNS)

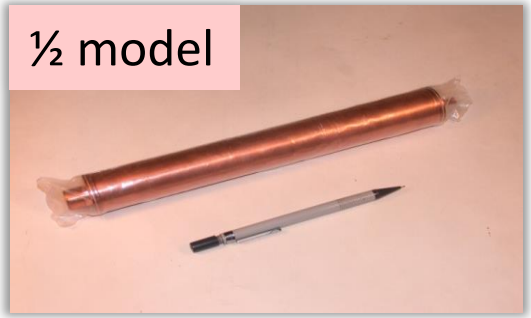

The basic design scheme of a tritium neutrino source (TNS) has been worked out in *A.A. Yukhimchuk et al. Fusion Science and Technology **48**, No.1 (2005) 731-736.*

Construction of a tubular tritium element

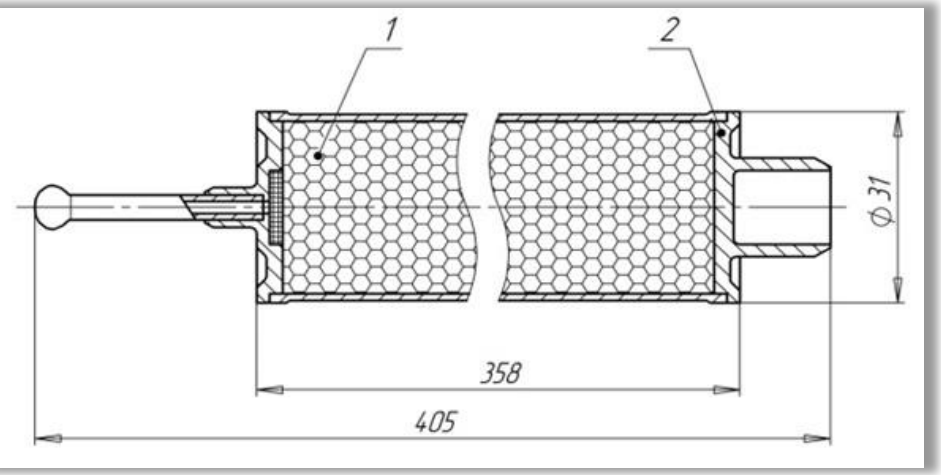

1 – titanium tritide; 2 – body

TNS is a set of tritium elements in which tritium is in a chemically bound state on titanium.

Titanium powder in bulk is placed in the tritium element. Then the titanium powder is thermally activated and saturated with tritium, after which the tritium element is sealed.

Quasiparticle readout: Quantum evaporation of He atom

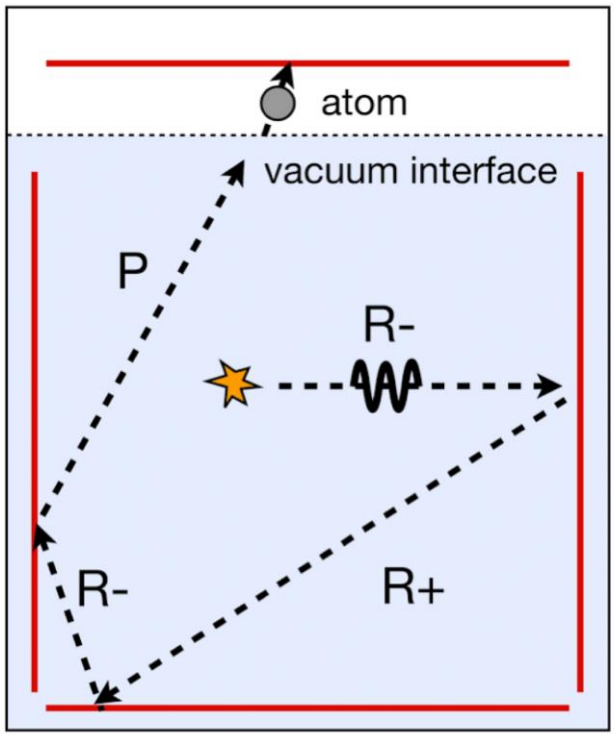

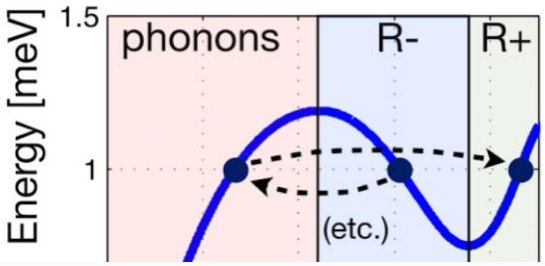

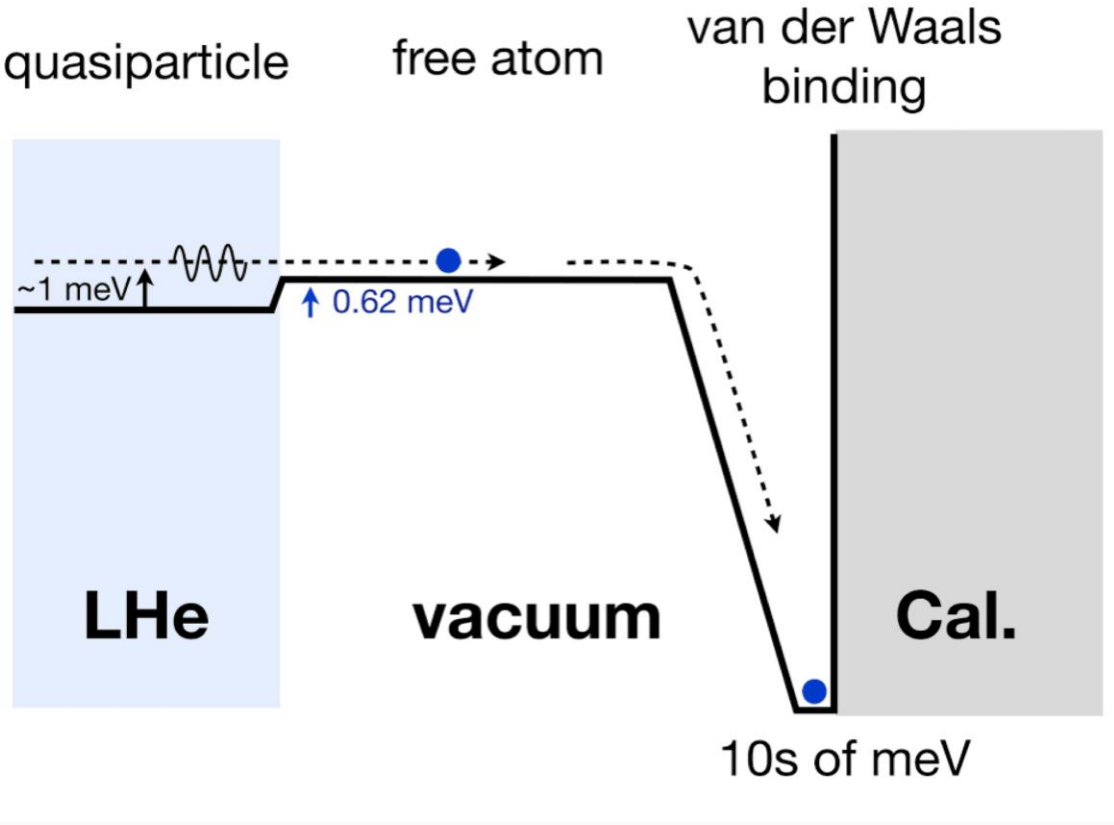

1 meV roton energy becomes up to 40 meV observable
- **x** 40 amplification
- Graphene-fluorine surface

[D. McKinsey, SNOLAB Workshop 2021]

The test He II cell for TRITON 200

@ JINR & Nizhny Novgorod State Technical University

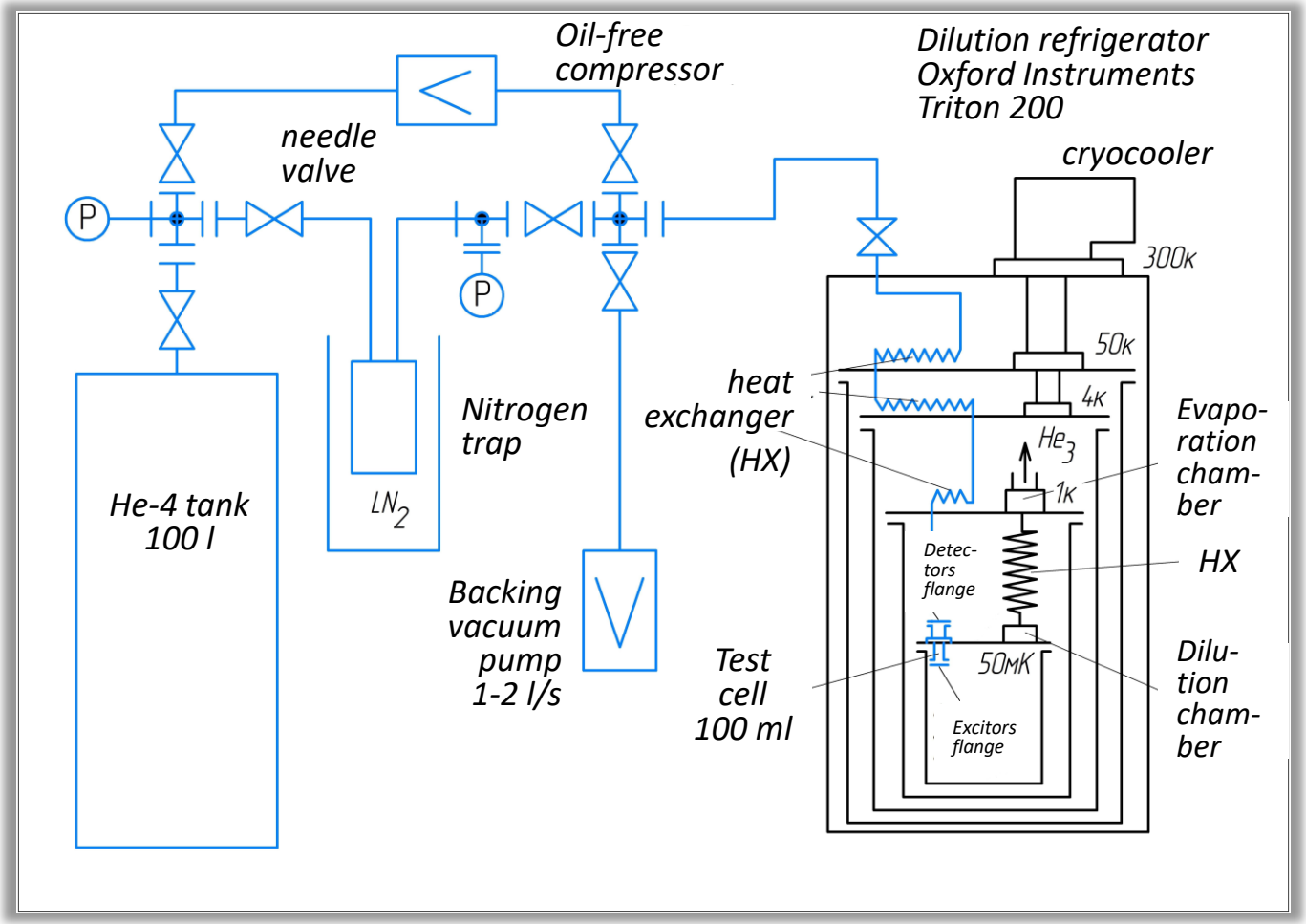

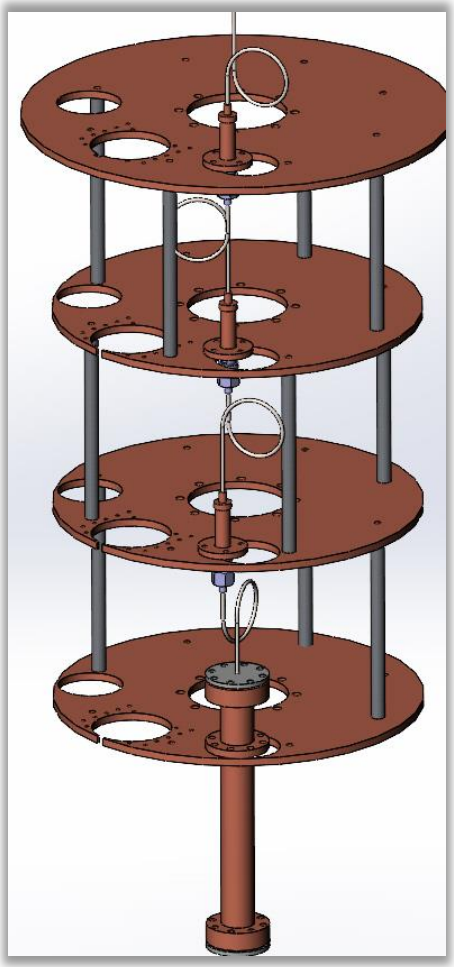

Purpose: To test the possibility of (i) generation of various excitations in helium (phonons, rotons, scintillations) by various controlled methods (thermal, mechanical, irradiation with various particles) and (ii) registration of these excitations by microcalorimetric detectors of various types

Transition edge sensor

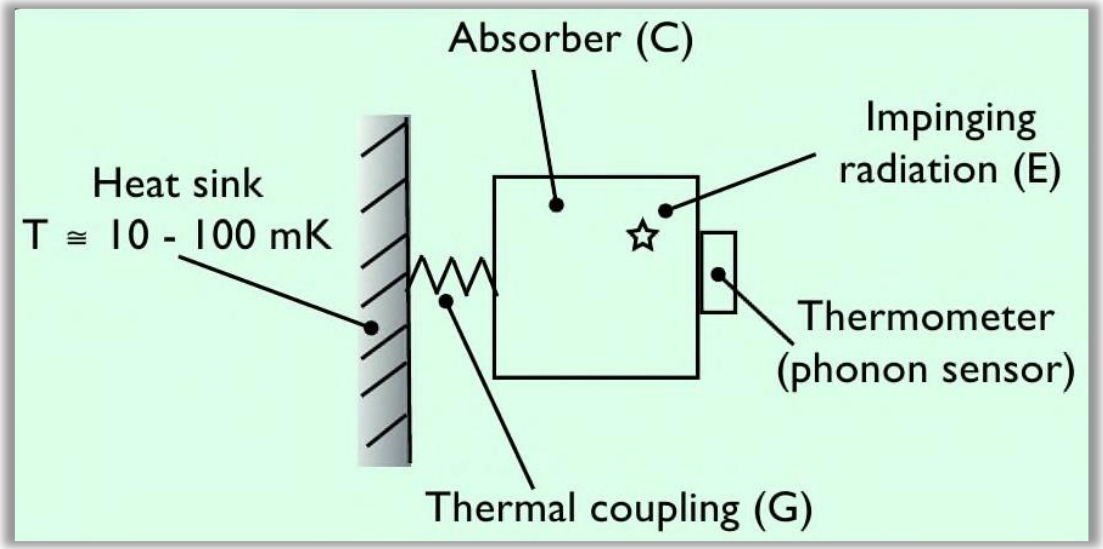

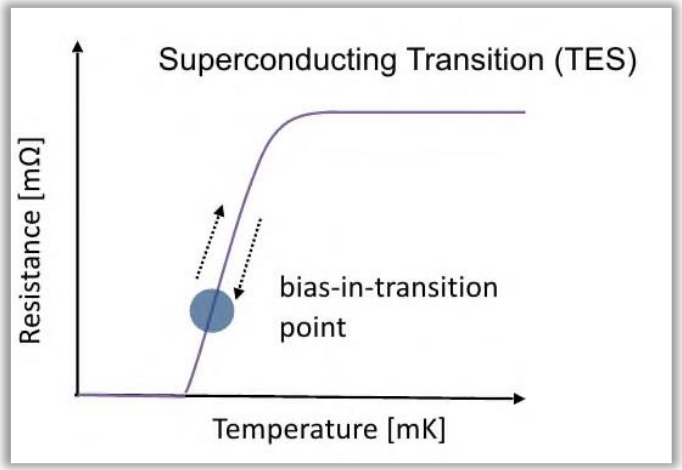

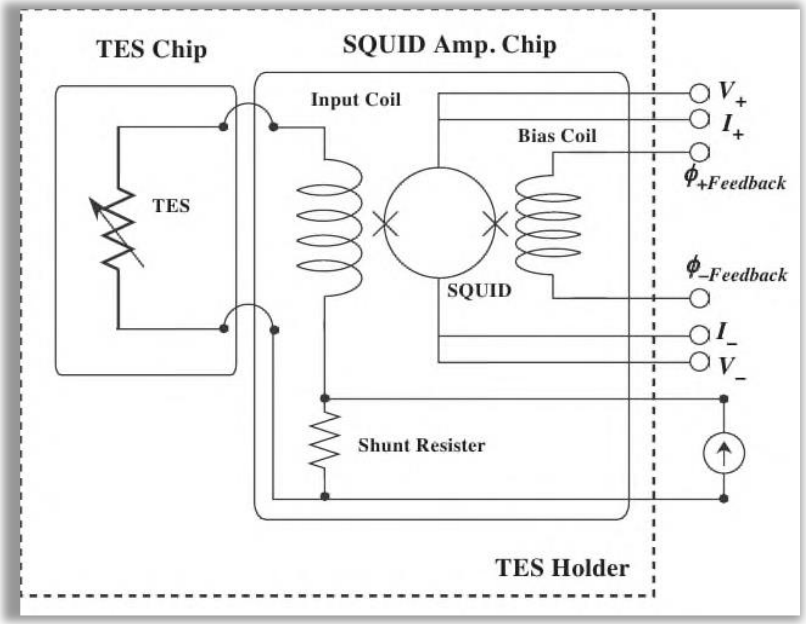

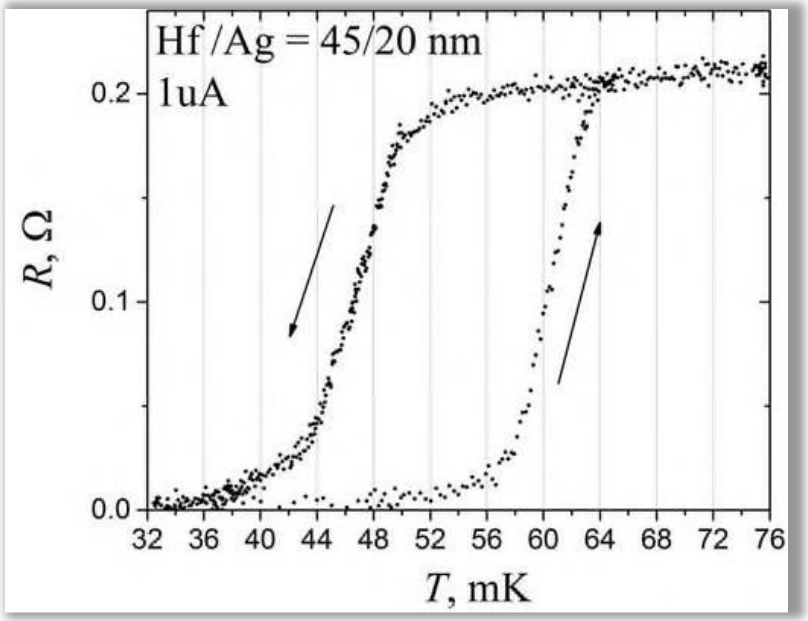

Thin-film metal structures for microcalorimeters

@ Institute for Physics of Microstructures, RAS, Nizhny Novgorod

Goal

Obtaining superconducting films with a critical temperature T_c from 15 mK to 100 mK and a sharp transition ΔT_c<1 mK

Methods and approaches

Multilayer structures with proximity effect:

Ti(T_c=0.49 K)/Mo(T_c=0.92 K)/Au & iridium films Ir (T_c = 0.11 K)

Allotropic modifications of tungsten: α-W(T_c=12-15 mK) / β-W (T_c=1-4 K)

Growth technologies

MOCVD with vertical reactor	MOCVD with horizontal reactor (EpiquipVP-502 RP)	Electron beam deposition (Amod 206)
		
α-W/Al_2O_3	α(β)–W/Al_2O_3; GaAs; Si	Ti/Mo/Au; Ir/Si

Post-growth and diagnostic methods

Ultraviolet lithography (Suss MJB4); Plasma etching (Oxford Plasmalab 8); X-Ray Diffractometry (BrukerD8 Discover); Secondary-ion mass spectrometry (TOF.SIMS-5); Atomic force microscopy

Studies of film electric properties

@ Nizhny Novgorod State Technical University

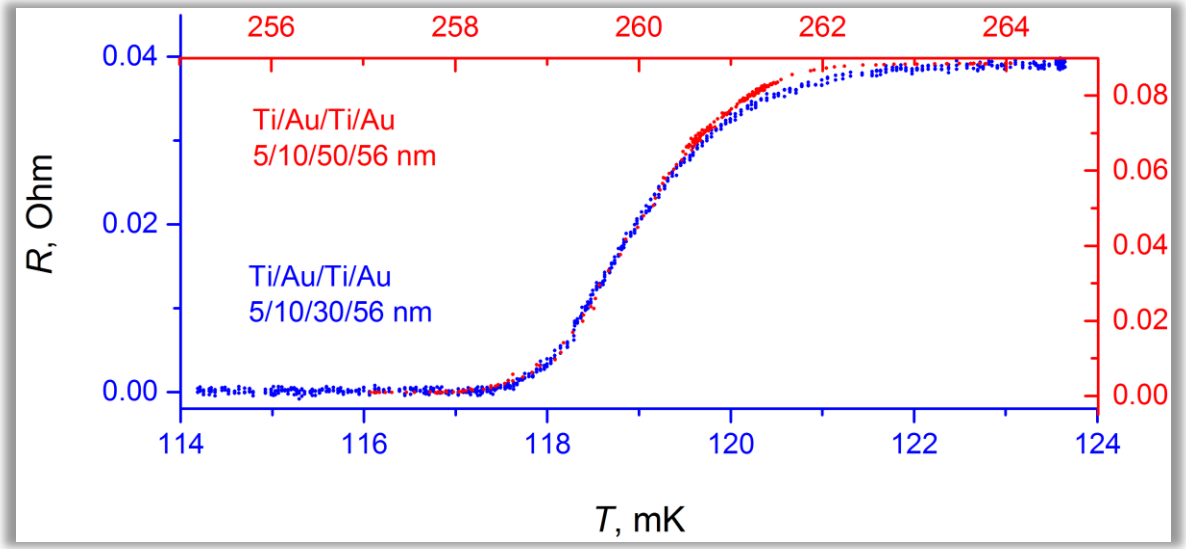

Neganov-Trofimov-Luke effect

Phonon amplification of ionization signal

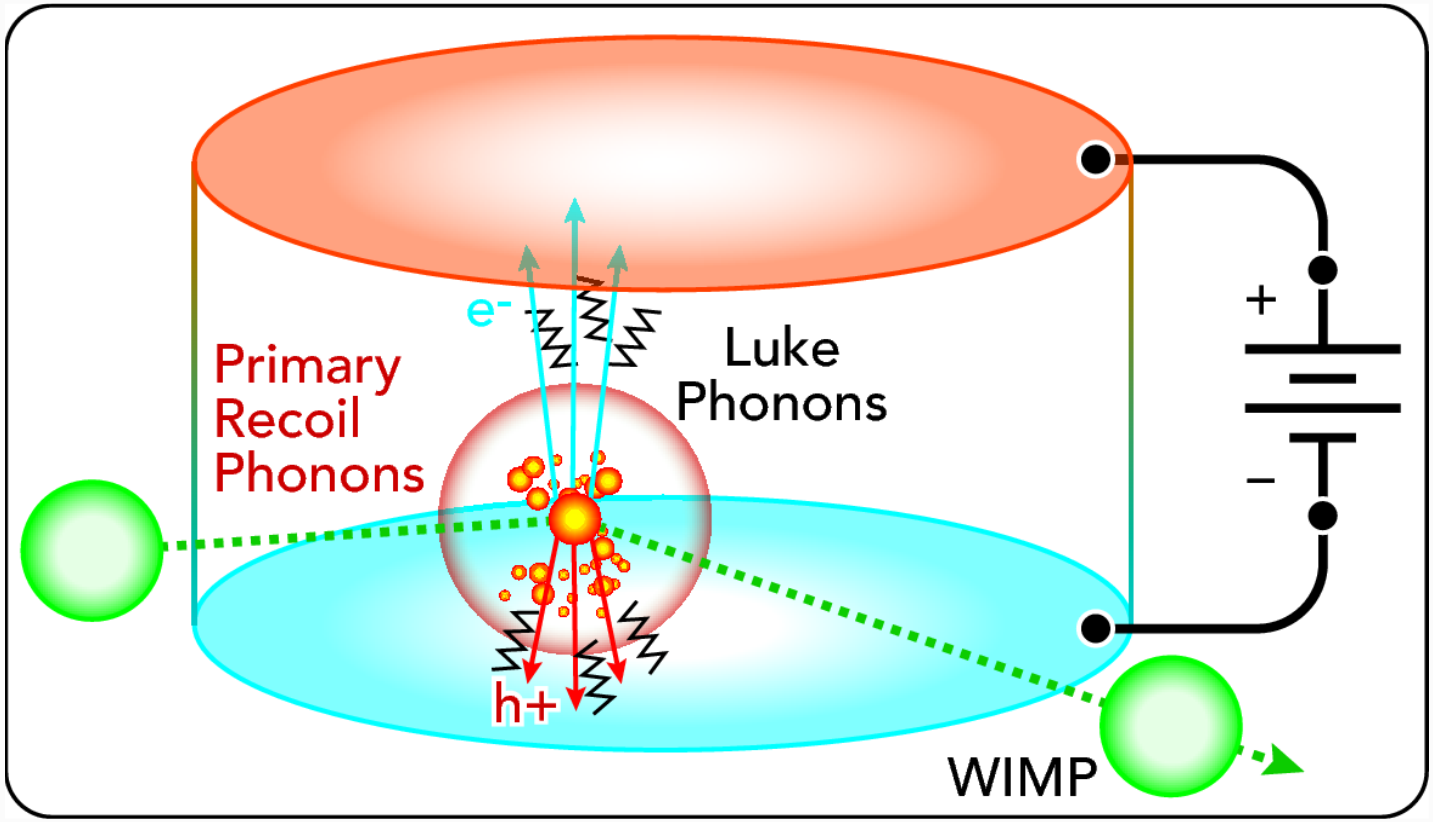

Observed Phonon Energy = $E_{Recoil} + E_{NTL}$

[B. von Krosigk (on behalf of the SuperCDMS Collaboration), IDM2018]

SuperCDMS detectors

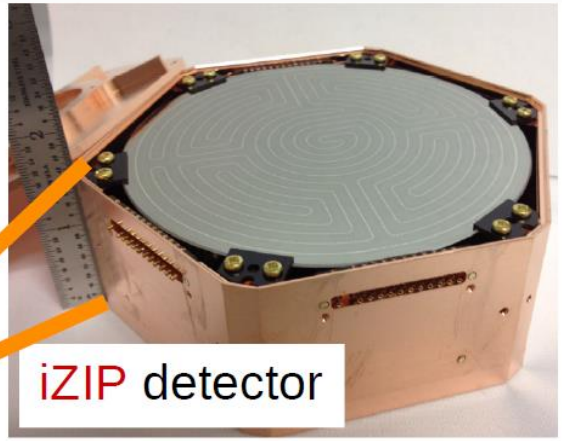

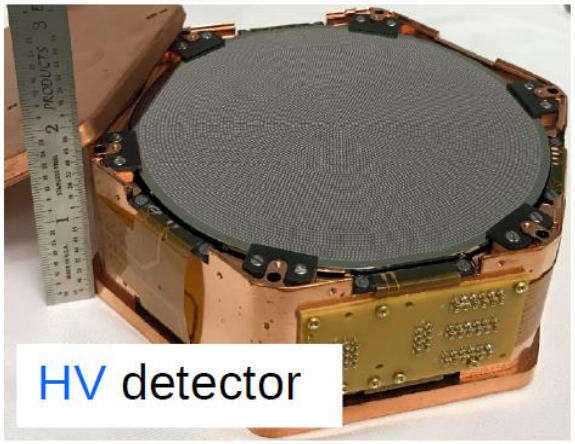

Ge detectors,
1.4 kg each.
Si detectors,
0.6 kg each.
Total: Ge: ~ 25 kg
Total: Si: ~ 3.6 kg

- High-purity Ge and Si crystals.
- Measurement of phonon signal via transition edge sensors.
- Bias voltage:
  - **iZIP**: < 10 V
    => Phonon + ionization signal
    => Nuclear / Electron Recoil discrimination.
  - **HV**: ~ 100 V
    => Phonon amplification of ionization signal
    => Very low threshold.

[B. von Krosigk (on behalf of the SuperCDMS Collaboration), IDM2018]

Prototype HVeV detector

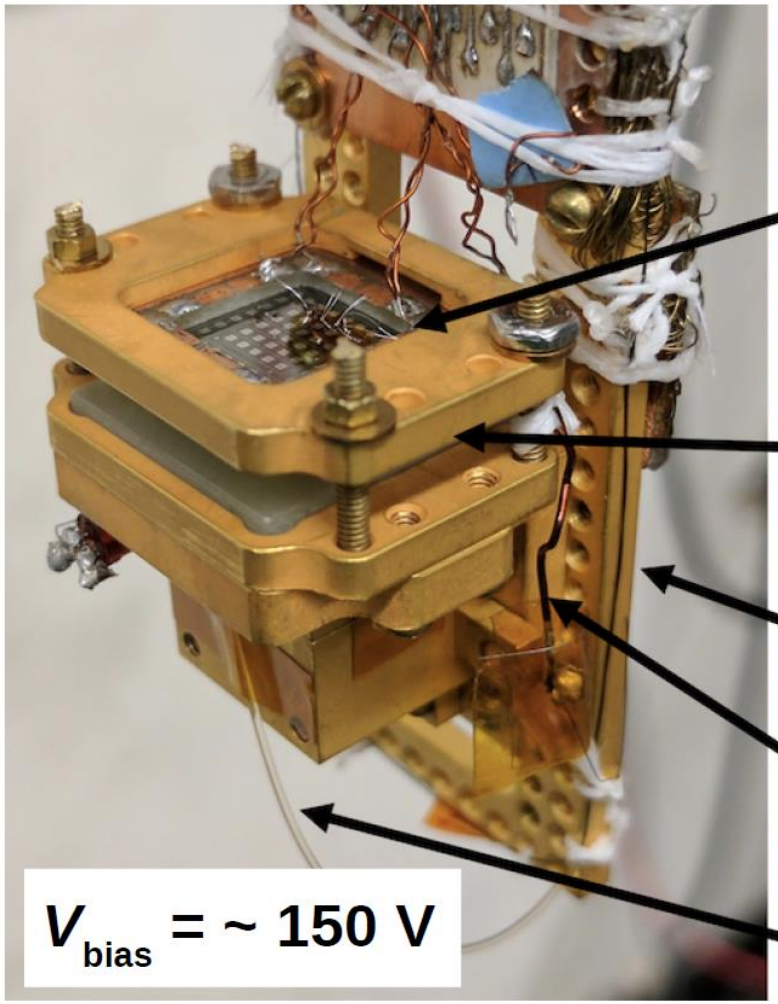

Si crystal (1cm^2 x 4mm, 0.93 g)
Phonon sensors

Crystal holder

Dilution refrigerator
sample stage (30 mK)

Bias voltage line

Fiber optic

- Strong NTL amplification of e^-h^+ pairs.
- Detector operated on surface at Stanford.

[B. von Krosigk (on behalf of the SuperCDMS Collaboration), IDM2018]

Prototype HVeV detector

- Si band gap: ~ 1.2 eV.
- Calibration data with pulsed 650 nm laser => 1.91 eV photons.

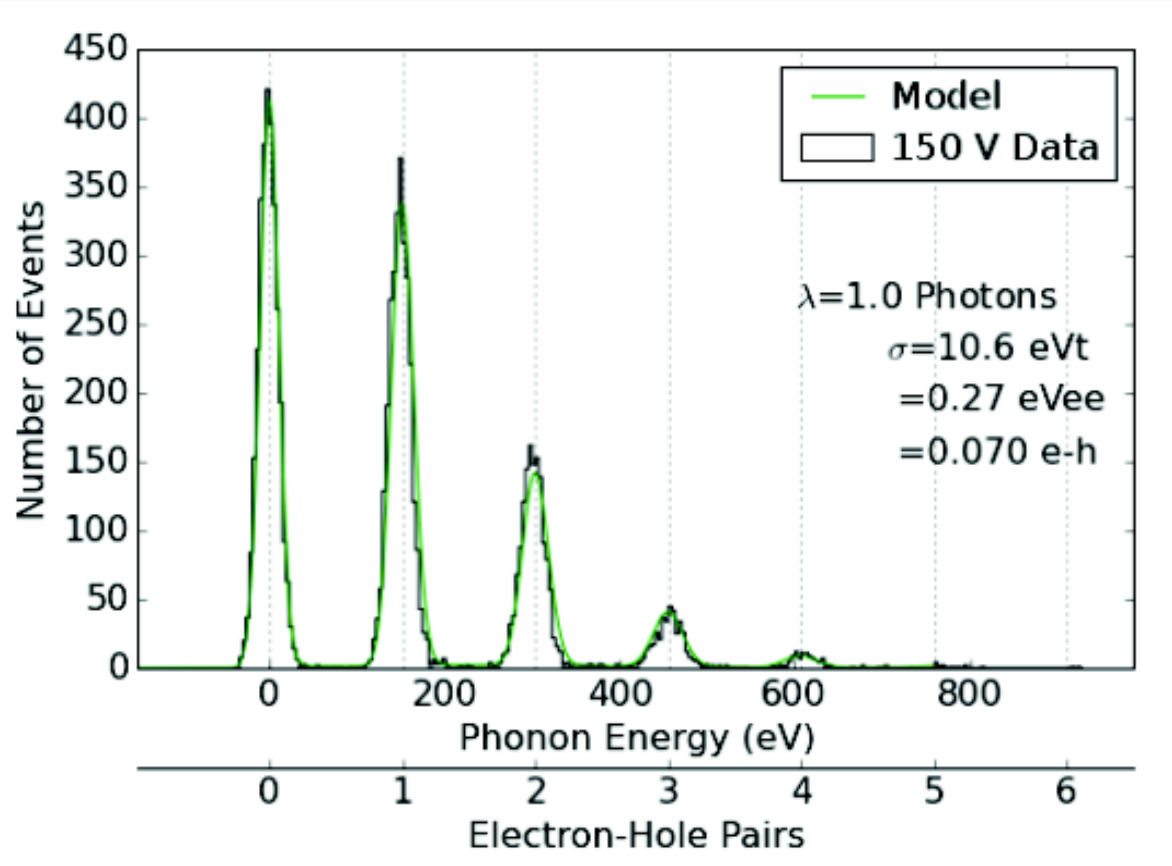

Sensitivity to single e^-h^+ pairs in Si crystal with a phonon sensor!

[B. von Krosigk (on behalf of the SuperCDMS Collaboration), IDM2018]

Testing parameters of CsI crystal modules

@ Institute of Nuclear Research, RFNC

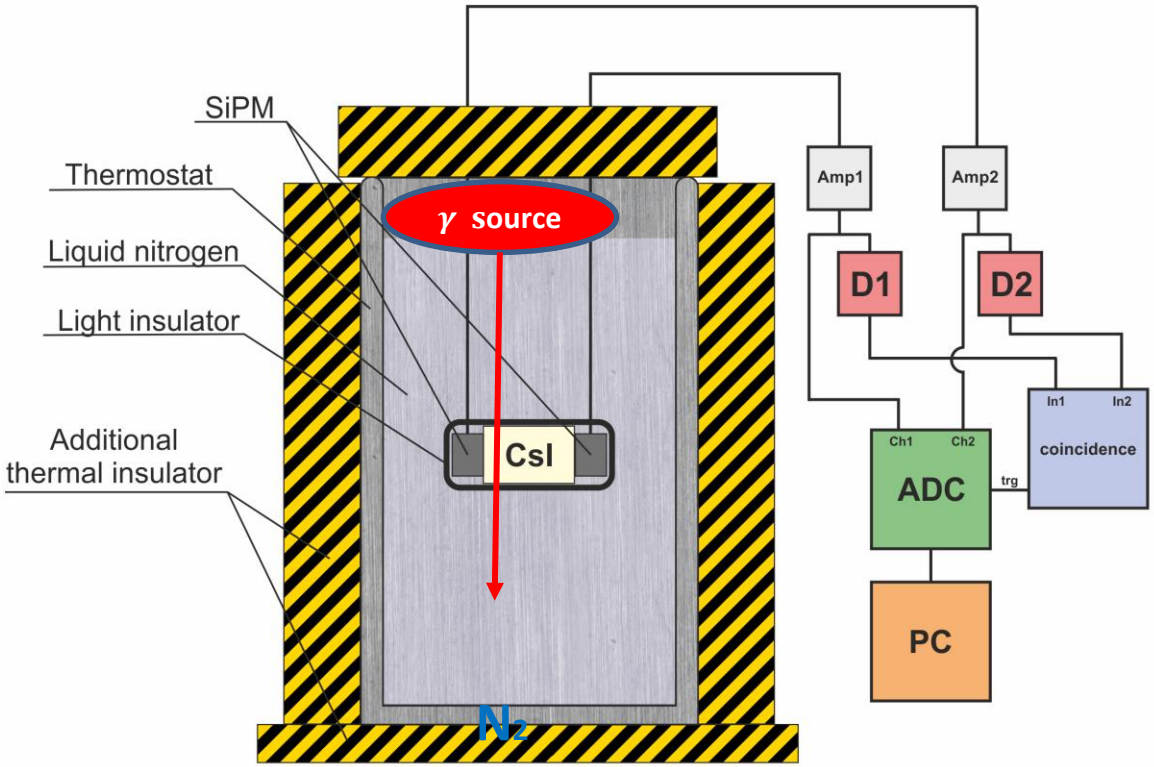

D1, D2 – discriminators (used in the coincidence scheme)

- CsI(pure) scintillation crystal is wrapped in Teflon tape.

- First tests were conducted with *one* and *two* SiPM readouts.

- Several γ sources were used to test modules in wide energy range (Am-241, Co-57, Cs-137, Na-22)

- CsI crystals of two different sizes were tested ($15 \times 15 \times 15\ \mathrm{mm}^3$ and $15 \times 15 \times 25\ \mathrm{mm}^3$)

1. The noise level of SiPM was measured at liquid nitrogen temperature.
2. Light collection was measured with CsI crystals of several sizes and with several types of analog signal amplifiers.
3. A maximum signal of 35 photoelectrons/keV was obtained, which is close to the expected level.

1st stable cryogenic operation of kg-scale pure-CsI crystal readout by SiPM arrays

L. Wang et al., Reactor neutrino physics potentials of cryogenic pure-CsI crystal, arXiv:2212.11515v1

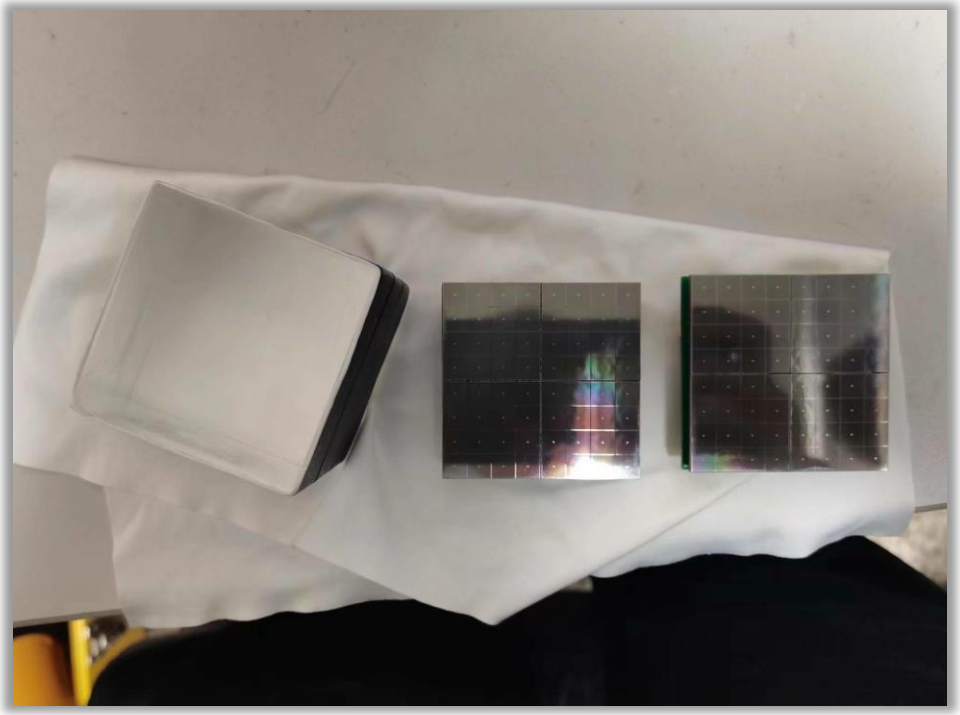

Fig. Main detector components:
one 2x2x2 inch^3 cubic pure CsI crystal
&
two Hamamatsu S14161-6050HS-4 22 SiPM arrays

A world-leading scintillation light yield among inorganic crystals was measured from a 0.5 kg pure-CsI detector operated at 77 K.

Scintillation photons were detected by two 2-inch Hamamatsu SiPM arrays equipped with cryogenic front end electronics.

A light yield of 52.1 phe/keV energy deposit was obtained for X-rays and γ-rays with energies from 5.9 keV to 60 keV.